Physiological outcomes of interleukin-6 in high fat diet and voluntary physical activity

A thesis presented to

The Faculty of Graduate Studies

of

Lakehead University

JESSICA SARVAS

In partial fulfillment of requirements

for the degree of

Master of Science in Biology

July 15th, 2014

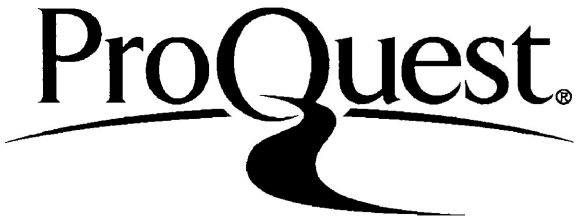

ABSTRACT

Insulin resistance is the principle step towards the progression of type 2 diabetes, and has been linked to increased circulating levels of cytokines, leading to chronic low-grade inflammation. Specifically, in chronic disease states increased interleukin-6 (IL-6) is thought to play a critical role in the regulation of insulin resistance in peripheral tissues, and has been used as a marker of insulin resistance. There is also an endogenous up-regulation of IL-6 in response to physical activity, which has been linked to improved insulin sensitivity. This leads to the question "how can elevated IL-6 lead to the development of insulin resistance, and yet also lead to increased insulin sensitivity?" Resolving the dual role of IL-6 in regulating insulin resistance/sensitivity is critical to the development of potential therapeutic interventions. This study was designed to investigate the role of IL-6 on high fat diet (HFD) induced glucose intolerance, and the response to voluntary physical activity in the prevention of insulin resistance. Six-week-old wild type (WT) and IL-6 knockout (KO) mice with (RUN) or without (SED) access to running wheels were fed a HFD (60% from kcal) for 4 weeks. A glucose tolerance test revealed that blood glucose levels were 25-30% higher in KO RUN compared to all other groups after 30 minutes. In WT RUN, weight gain was positively correlated with total caloric intake; however, this correlation was absent in KO RUN, which may be attributed to impaired glycogen breakdown or increased thermogenesis in these mice. In soleus muscle, there was a 2-fold increase in SOCS3 expression in KO RUN compared to all other groups. In gastrocnemius/plantaris muscles, Akt phosphorylation was 31% higher in WT RUN compared to WT SED, but this effect of running was absent in KO mice.

Additionally, there was a 2.4-fold increase in leptin expression in KO RUN compared to KO SED in the gastrocnemius/plantaris muscles. In the liver, there was a 2-3.8-fold increase in SOCS3 expression in KO SED compared to all other groups, and AMPKα phosphorylation was 27% higher in WT mice (both RUN and SED) compared to KO mice (both RUN and SED). These findings provide new insight into the role of the IL-6 in metabolism and energy storage, and highlights tissue specific changes in early signaling pathways in response to HFD for 4 weeks. The collective findings suggest that endogenous IL-6 is important for the prevention of insulin resistance leading to type 2 diabetes.

LAY SUMMARY

Faculty and students in the Department of Biology are bound together by a common interest in explaining the diversity of life, the fit between form and function, and the distribution and abundance of organisms. The purpose of this research was to investigate the effects of the cytokine IL-6, high fat diet, and physical activity on glucose tolerance and insulin action within a more physiological context. The findings suggest that IL-6 is important for the prevention of insulin resistance induced by high fat diet, and help further our understanding of the mechanisms behind the increase in insulin sensitivity in response to regular physical activity in the treatment and prevention of type 2 diabetes.

DEDICATION

To my family and friends for their love, patience, and support.

ACKNOWLEDGEMENTS

First and foremost I would like to thank both Dr. Simon Lees, and Dr. Neelam Khaper for their key roles as my mentors and thesis co-supervisors. Thank you for trusting me to help plan and design the direction and experiments of my project. This opportunity allowed me to become invested in the research, and kept me motivated to make this project a success. Thank you for everything that both of you have taught me along the way, from the animal experiments and lab techniques, to presentation skills and title writing. The past two years would not have been possible without your knowledge, guidance, encouragement, and "tough love" to keep me on track.

I would also like to thank my committee member Dr. Dave Law, for his knowledge and support of my project.

Thank you to all the Northern Ontario School of Medicine (NOSM) students, scientists, and employees. You have all provided me with an atmosphere of respect, and constant learning and collaboration. I would also like to thank my fellow lab member Sarah Niccoli for helping me every step of the way. I am truly lucky to have had the opportunity to seek advice from, and work with someone who is so dedicated and passionate about research.

Table of Contents

LIST OF TABLES

LIST OF FIGURES

LIST OF ABBREVIATIONS

AMPK	AMP activated protein kinase
BAT	Brown adipose tissue
GLUT-4	Glucose transporter 4
HFD	High fat diet
IR	Insulin receptor
IRS-1/IRS-2	Insulin receptor substrate 1 and 2
IL-6	Interleukin-6
KO	Interleukin-6 knockout
PI3K	Phosphoinositide 3 kinase
STAT3	Signal transducer and activator of transcription 3
SOCS3	Suppressor of cytokine signalling 3
T2D	Type 2 diabetes
UCP	Uncoupling proteins
WAT	White adipose tissue
WT	Wild type

INTRODUCTION

It is estimated that 347 million people worldwide have diabetes, with approximately 90% of those cases being type 2 diabetes (T2D) (World Health Organization). There are many grave pathophysiological outcomes of T2D, leading to increased morbidity and mortality. Increased blood glucose levels associated with T2D leads to a greater incidence of tissue damage leading to complications in the cardiovascular system, kidneys, retina, and peripheral nervous system. Furthermore, the World Health Organization projects that deaths attributed to diabetes will double between 2005 and 2030. Altered function of insulin at peripheral tissues leads to insulin resistance in skeletal muscle, liver, and adipose tissue, which is critical to the development and progression of T2D.

Insulin is an anabolic hormone that is released by the β-cells in the pancreas to maintain glucose homeostasis within the body. The insulin-signaling cascade begins when insulin binds to the insulin receptor (IR) on the cell membrane. Insulin binding results in autophosphorylation and activation of the IR beta subunit. Once activated, IR phosphorylates and activates several molecules, including the insulin receptor substrate (IRS) proteins 1 and 2. IR binds to IRS-1 and IRS-2 through the Pleckstrin Homology (PH), and Phosphotyrosine Binding (PTB) domains [1]. IRS-1 functions primarily in skeletal muscle and adipose tissues, whereas IRS-2 functions primarily in the liver [2]. The tyrosine phosphorylation of IRS proteins activates binding sites for Src homology 2 (SH2) domain proteins including phosphoinositide 3-kinase (PI3K) [3]. IRS phosphorylates PI3K by binding to the regulatory subunit p85, and generates membrane

phosphatidyl-inositol-3,4,5-trisphosphate (PIP3). In turn, PIP3 recruits and activates phosphoinositide 3-dependent kinase 1 and 2, protein kinase C, and Akt leading to subsequent phosphorylation of downstream targets such as mammalian target of rapamycin (mTOR), and glycogen synthase kinase-3β. Insulin is released in response to increased levels of circulating glucose, causing a coordinated response in peripheral tissues with the overall goal to take up and store glucose. Insulin stimulates glucose uptake in skeletal muscle and adipose tissue, and the activation of Akt causes translocation of glucose transporter 4 (GLUT-4) vesicles to the plasma membrane to facilitate glucose transport into the cells. In the liver, insulin signaling regulates gluconeogenesis by inhibiting key enzymes, resulting in reduced hepatic glucose output. Although skeletal muscle accounts for approximately 75% of whole body insulin-stimulated glucose uptake through both insulin dependent and insulin independent mechanisms, glycogen synthesis is also stimulated to store large amounts of glucose in the liver [4]. The effects of insulin on glucose metabolism are complex and highly regulated. Adding to this complexity, these signaling pathways can be altered or influenced by various pathophysiological conditions, such as inflammation, infection, and obesity.

The current literature provides evidence that elevated IL-6 plays an important role both in the development of insulin resistance, and as a mediator of physical activity induced increases in insulin sensitivity. Therefore, an IL-6 paradox does exist, such that elevated IL-6 can lead to the development of insulin resistance, and yet can also lead to increased insulin sensitivity. However, there are still many gaps in the knowledge related to these

context dependent physiological outcomes of elevated IL-6. An improved understanding of the mechanisms behind IL-6 signaling, physical activity, and insulin sensitivity are required to develop improved treatment strategies for T2D.

Chronic low-grade inflammation *versus* acute inflammation

Interleukin-6 (IL-6) is a pleiotropic cytokine that is secreted by and acts on a wide variety of tissues and cells. IL-6 mediates several steps in the activation of inflammatory responses, by regulating the synthesis of pro-inflammatory cytokines [5]. However, IL-6 also promotes the synthesis of anti-inflammatory cytokines such as, IL-1 receptor antagonist and IL-10 [5,6]. Therefore, IL-6 exhibits both pro- and anti-inflammatory properties, and there seems to be context dependent effects. The plasma levels of IL-6 in healthy humans are typically less than 5 pg/ml [7] (Table 1). Although many different cell types are capable of producing IL-6, the release differs under varying physiological conditions within the body. In healthy humans, adipose tissue releases 10-35% of IL-6 in basal circulating levels [8]. Immune cells, specifically macrophages, that are present within adipose tissue are responsible for releasing the majority of IL-6 from this tissue [9]. In obesity, increased numbers of macrophages begin to infiltrate the white adipose tissue, and the macrophage content correlates positively with adiposity and adipocyte size [10]. This increased number of macrophages leads to increased production of C-reactive protein, and inflammatory cytokines, including TNFα, IL-1β and IL-6 [11]. Additionally, it was found that TNFα and IL-6 were more highly expressed in macrophages compared to adipocyte cells in adipose tissue obtained from an obese mouse model (*ob/ob*). Therefore, obesity has been characterized as a state of chronic low-grade inflammation,

due to the increased secretion and subsequent ~2-3-fold elevation in systemic inflammatory markers from macrophages in the adipose tissue [10,12] (Table 1).

In contrast to chronically elevated IL-6, there can also be elevated IL-6 in response to acute infection, sepsis or physical activity. An acute phase response results in the release of similar inflammatory markers that are seen in chronic low-grade inflammation, however, the acute circulating levels of these markers are much higher than levels associated with systemic inflammation. An acute transient increase in inflammatory markers also occurs during physical activity [11]. While it is true that eccentric contractions cause damage to skeletal muscle and can elicit an inflammatory response, there is also an acute transient increases in cytokine levels in response to physical activity in undamaged muscle [13]. However, unlike sepsis and infection, pro-inflammatory cytokines, TNFα and IL-1β, do not typically increase [14,15]. It has been reported that plasma IL-6 concentrations increased approximately 100 fold during exercise, and the magnitude of increase in IL-6 depends on the duration and intensity of the exercise [16-18] (Table 1). Increases in IL-6 mRNA and protein were found in skeletal muscle during exercise, and the skeletal muscle cells produced enough IL-6 to account for the large increase in plasma IL-6 levels [19-21]. In contrast to chronic low-grade inflammation, infection and sepsis, it was shown that this acute increase in IL-6 levels was not due to activation of macrophages [22].

Table 1. Plasma levels of inflammatory markers in humans under varying physiological and pathophysiological conditions.

Inflammatory Marker[1]	Normal	Obesity	Sepsis	Exercise
IL-6	<5 pg/ml [7,12,97,103-109]	1.5-38 pg/ml [105,106,110-113]	3.5-16000 pg/ml [115,116]	~100 fold elevation in resting concentration [6,16-18,97]
TNF-α	<3.5 pg/ml [12,16,103,106,116]	1.8-88 pg/ml [106,110,113]	Undetectable-1000 pg/ml [117]	~2 fold elevation in resting concentration [6, 16]
IL-10	<3.0 pg/ml [103,109,118]	0.35-10 pg/ml [108,111,112,118]	Undetectable-1700 pg/ml [119]	~8-27 fold elevation in resting concentration [6,16]
CRP	<10 mg/l [107]	1.3-8.5 mg/l [105,106,108,110,112]	>10 mg/l [120]	Up to 100 fold elevation in resting concentration [6,16,121]

[1] IL-6=interleukin-6, TNF- α=tumor necrosis factor alpha, IL-10=interleukin-10, CRP=C reactive protein

Although both chronic low-grade inflammation and physical activity result in increased plasma IL-6 levels, there are important differences between the two conditions. Chronic low-grade inflammation is characterized by a slight yet significant systemic increase in IL-6 levels, whereas physical activity results in an acute and transient increase in IL-6 levels. During chronic low-grade inflammation the increased IL-6 is released primarily from macrophages in adipose tissue [10,12], while during physical activity the IL-6 is released from skeletal muscle [19,23]. IL-6 released from muscle during physical activity allows accumulation within the skeletal muscle compartment and potentially increases specificity of IL-6 signaling at skeletal muscle, acting in an autocrine/paracrine fashion. This also may account for differences observed in the effects of IL-6 in response to physical activity (acute/transient) versus chronic low-grade inflammation. Although IL-6 released from skeletal muscle still ends up in the circulation, and acts in an endocrine manner during physical activity, the elevated IL-6 is only transient, and therefore, does not have the negative effects on tissues seen with chronically elevated IL-6 levels. The differences between these chronic and acute IL-6 elevations may be important with respect to the effects that the increased IL-6 has on target tissues, and more specifically, the effects on insulin signaling within these tissues.

IL-6 increases SOCS3 expression

IL-6 initiates cell signaling by binding to the IL-6 receptor (IL-6R), which is also known as a type I cytokine receptor. The IL-6R exists as membrane bound and soluble receptors, and IL-6 regulates the inflammatory state by coordinated signaling through both forms. The interaction between IL-6 and IL-6R forms a heterodimer with a non-ligand binding membrane glycoprotein, gp130 [24]. The complex formed between IL-

6/IL-6R and gp130 activates the Janus kinase-signal transducer and activator of transcription (Jak/STAT) signal transduction pathway in IL-6 target cells, leading to the phosphorylation of the cytoplasmic portion of gp130 [25]. The phospho-tyrosine residues on gp130 are docking sites for STAT proteins, which are able to bind to these docking sites via SH2 (Src-homology 2) domains. Several studies, both *in vitro* and *in vivo*, have shown that IL-6 stimulation increases the phosphorylation of STAT3 proteins. Activated STAT3 is translocated to the nucleus, where it is able to regulate the transcription of IL-6 target genes. IL-6 mediated Jak/STAT signaling can be induced rapidly, and results in increased phosphorylation of STAT3 under acute inflammatory conditions [26-29] (Fig. 1).

As a negative feedback control, activated STAT proteins induce the expression of suppressor of cytokine signaling (SOCS) proteins, which inhibit signaling events in response to various cytokines, including IL-6, IL-10, and interferon gamma. SOCS3 is able to down regulate IL-6 signaling by exerting negative feedback control on the Jak/STAT pathway through various mechanisms [30-32]. Both *in vivo* and *in vitro* studies provide evidence that elevated circulating levels of IL-6 result in increased expression of SOCS3 proteins in skeletal muscle [26,33-35], liver [36], and adipose tissue [26,37]. Consequently, this increase in SOCS3 expression has various important downstream effects on the insulin-signaling pathway in these tissues.

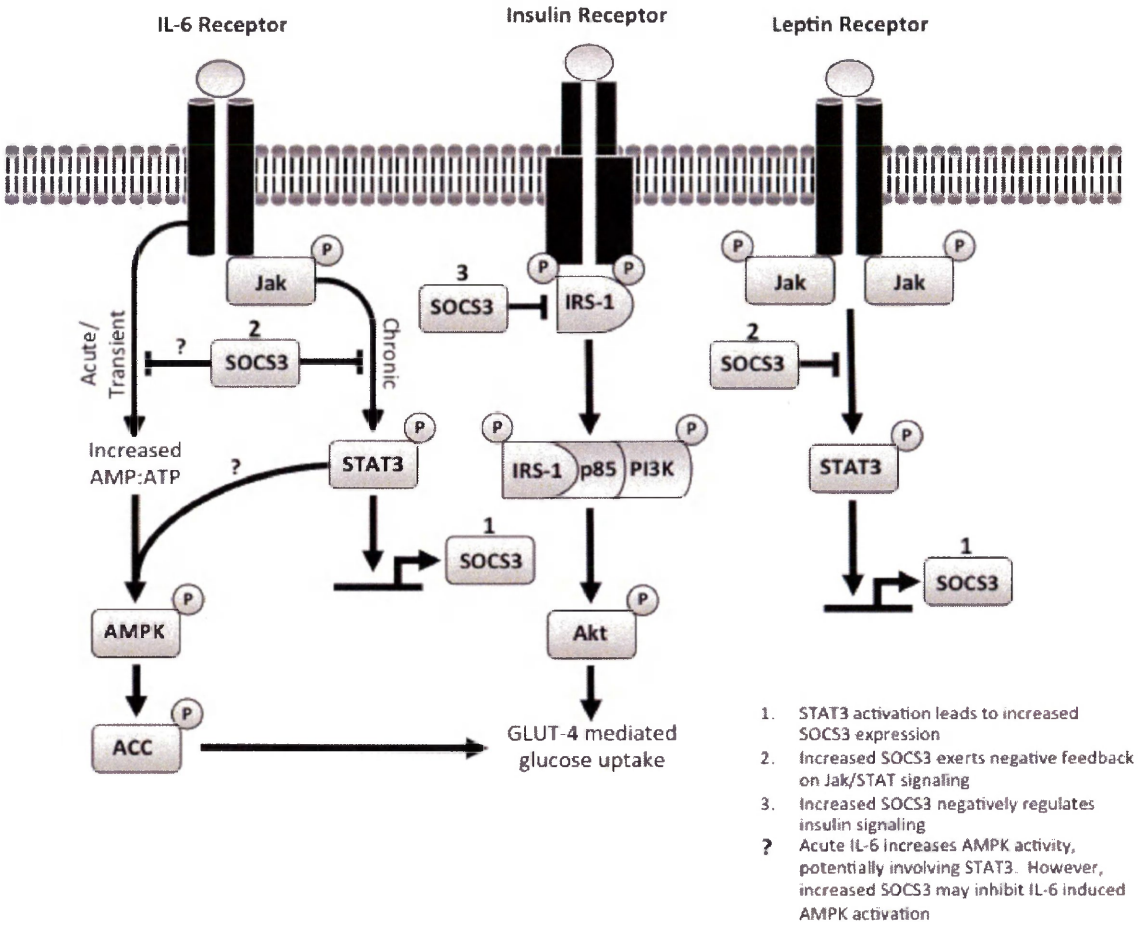

Figure 1. IL-6, insulin, and leptin signaling in skeletal muscle. Chronic low-grade inflammation is associated with increased levels of IL-6, which leads to increased phosphorylation of STAT3, and subsequent increased SOCS3 expression. Increased SOCS3 mediates the inhibitory effects of IL-6 on insulin signaling and glucose uptake. SOCS3 directly disrupts insulin signaling by binding to IR and preventing interaction with IRS-1 (primarily in skeletal muscle and adipose tissue) / IRS-2 (primarily in the liver), and may target IRS-1/IRS-2 for degradation. Disrupting the early signaling events also has downstream effects on other proteins in the insulin pathway including PI3K and Akt, ultimately leading to insulin resistance and attenuated GLUT-4 mediated glucose uptake. Chronically elevated leptin levels also leads to increased SOCS3 expression,

which can also directly inhibit insulin mediated glucose uptake. In addition, SOCS3 can have indirect effects on glucose uptake; increased SOCS3 leading to leptin resistance, and impaired leptin mediated AMPK activation. In contrast, acute/transient IL-6 elevations in response to physical activity do not cause sustained increased SOCS3 expression, but cause increased insulin sensitivity in peripheral tissues by increased AMPK activity and subsequent increased glucose uptake. IL-6 mediated activation of AMPK in response to physical activity is blunted in chronic inflammatory states. Since IL-6 is required for physical activity-induced AMPK activation and obesity results in a blunted physical activity-induced activation of AMPK, it is possible that increased SOCS3 may cause IL-6 resistance, which results in diminished AMPK activity and increased insulin resistance.

IL-6=interleukin-6, STAT3= signal transducer and activator of transcription 3, SOCS3=suppressor of cytokine signaling 3, IR=insulin receptor, IRS=insulin receptor substrate, PI3K= phosphoinositide 3 kinase, GLUT-4=glucose transporter 4, AMPK=AMP activated protein kinase

SOCS3 and insulin resistance

Chronically elevated IL-6 leads to increased expression of SOCS3 proteins in skeletal muscle, liver and adipose tissue. This increased expression of SOCS3 mediates the inhibitory effects of IL-6 on insulin signaling and glucose metabolism [36,38,39]. It has been shown that insulin resistance increases following SOCS3 adenoviral [36] and transgene [38] overexpression in liver and adipose tissue. SOCS3 adenoviral overexpression in the liver of *db/db* obese mice lead to increased plasma insulin concentrations, glucose intolerance, and insulin resistance. Furthermore, when these mice were given antisense treatment for SOCS3 protein, insulin sensitivity improved [39]. Similarly, after a muscle specific deletion of SOCS3, whole body glucose tolerance and insulin sensitivity increased. This was due to enhanced glucose uptake into skeletal muscle [40]. Additionally, it was found that insulin sensitivity increased following an adipose tissue specific SOCS3 deletion, suggesting that SOCS3 negatively regulates insulin signaling [37,41]. Although it has been demonstrated that increased SOCS3 expression causes insulin resistance in multiple tissues, the mechanisms by which SOCS3 exerts these effects are less clear. There is a large body of evidence supporting that SOCS3 disrupts insulin signaling by binding to specific sites on IR, and IRS-1/IRS-2, as well as targeting IRS-1/IRS-2 for degradation [36]. Disrupting these early signaling events also has downstream effects on other important proteins in the insulin pathway, including PI3K and Akt.

It has been demonstrated that the β subunit of IR and SOCS3 co-immunoprecipitated in muscle lysates, and adenoviral mediated overexpression of SOCS3 resulted in decreased

insulin stimulated phosphorylation of both IRS-1 and IRS-2 [36]. Since the decreased phosphorylation of IRS-1 and IRS-2 occurred without a decrease in IR phosphorylation, SOCS3 may bind to residues on IR that are involved in IR/IRS binding. Tyrosine 960 of IR is an important residue in IR/IRS binding [42], and when mutated to phenylalanine, SOCS3 was unable to bind to the β subunit of IR [36]. This finding suggests that when SOCS3 binds to the IR, it inhibits IR/IRS1 interaction, and consequently, disrupts insulin signaling. Co-immunoprecipitation of SOCS3 with both the β subunit of IR and IRS-1 was increased in skeletal muscle from rats fed HFD and obese Zucker rats compared to the control rats [43,44]. HFDs cause elevated IL-6, which leads to increased SOCS3 expression, and acts as barrier between IR and IRS-1 binding. Consequently, insulin stimulated tyrosine phosphorylation of IRS-1 was decreased in both the HFD rats and obese Zucker rats compared to the control rats [43,44]. The decreased IRS-1 phosphorylation caused decreased activity and phosphorylation of PI3K, and increased insulin resistance [44]. Following a skeletal muscle specific SOCS3 deletion, there was no difference in IR, IRS-1, and Akt protein expression. However, IRS-1 association with the p85 subunit of PI3K and Akt phosphorylation increased in SOCS3 deficient mice after insulin stimulation [40]. These studies suggest that muscle specific SOCS3 deletion improves insulin sensitivity in mice fed a HFD.

Along with skeletal muscle, increased SOCS3 expression can also induce insulin resistance in the liver. When the HepG2 cells (human liver cell line) and primary hepatocytes were treated first with IL-6 and then insulin, SOCS3 expression increased, and tyrosine phosphorylation of IRS-1 and IRS-2 were decreased, but the

phosphorylation of IR did not differ [45,46]. Similar to skeletal muscle, it was found that SOCS3 co-immunoprecipitated with the β subunit of IR in liver lysates, and these findings suggest that SOCS3 attenuates insulin signaling by inhibiting IR/IRS binding in the liver [36]. Increased SOCS3 suppressed IRS-1 association with the p85 subunit of PI3K, and attenuated Akt phosphorylation [39,45,46]. When treated with antisense oligonucleotides against SOCS3, the phosphorylation of both IRS-1 and IRS-2 was restored, and the activity of PI3K and Akt was improved [39]. In a lipopolysaccharide (LPS) model for sepsis, SOCS3 protein expression was increased in the liver, which resulted in a drastic decrease in IRS-1 and IRS-2 phosphorylation in response to insulin. Furthermore, insulin stimulated PI3K and Akt activity were both significantly decreased [36]. However, in contrast to other studies, IR phosphorylation was decreased in the mice that were treated with LPS. It should be noted that LPS injection simulates endotoxemia in the liver tissue, and this is a severe model of systemic inflammation compared to chronic low-grade inflammation. This may account for discrepancies in results between studies using these different models of inflammation.

In addition to decreased tyrosine phosphorylation of IRS-1 and IRS-2, SOCS has also been shown to mediate the degradation of these proteins. Adenoviral mediated expression of SOCS1 in liver lysates resulted in reduced levels of IRS-1 and IRS-2 proteins, and these levels returned to normal when SOCS1 was no longer detected [47]. SOCS proteins contain a highly conserved binding domain known as the SOCS box [30-32]. The SOCS box has an Elongin C binding motif that can form a complex with Elongin B [48]. This Elongin BC complex assembles an E3 ubiquitin ligase complex,

which can degrade IRS-1 and IRS-2 proteins [49]. The deletion of SOCS box residues resulted in no reduction of IRS-1 and IRS-2 proteins levels when SOCS1 was expressed using an adenovirus [47]. Although these results were only shown with SOCS1, the Elongin C binding motif is present in the SOCS box of both SOCS1 and SOCS3. Therefore, under certain circumstances degradation via the E3 ubiquitin ligase complex is a plausible explanation for the reduced IRS-1 and IRS-2 protein levels following SOCS3 expression [36].

Along with skeletal muscle and liver, SOCS3 is also a negative regulator of insulin signaling in adipose tissue. When SOCS3 was overexpressed in primary adipocytes or adipose tissue, insulin stimulated IRS-1 tyrosine phosphorylation, PI3K activation of p85 subunit, and Akt phosphorylation decreased resulting in increased insulin resistance [38,50]. There was also a significant reduction in IRS-1 protein levels, which suggests that SOCS3 may be capable of degrading IRS-1 via ubiquitin ligase in adipose tissue [38,50]. SOCS3 deficient mouse embryonic fibroblasts, differentiated into adipocytes, showed increased IRS-1 and IRS-2 tyrosine phosphorylation compared to wild type adipocytes when stimulated with insulin [37]. Additionally, in the SOCS3 deficient adipocytes, p85 subunit binding to IRS-1, PI3K activity, and glucose uptake were all increased. During chronic insulin treatment, which simulates conditions that lead to increased SOCS3 expression, IRS-1 protein levels were decreased in wild type adipocytes, which were not seen in the SOCS3 deficient adipocytes [37]. HFD mice with an adipose tissue specific deletion SOCS3 deletion (AKO) had increased glucose infusion rate with hyperinsulinaemic-euglyceamic clamp tests compared to the control mice [41].

Following a bolus of insulin, there was decreased IRS-1 tyrosine phosphorylation and IRS-1 protein levels in the HFD control mice compared to the HFD AKO mice. These findings demonstrate that the deletion of SOCS3 can protect against HFD induced insulin resistance in adipose tissue.

Collectively, these studies provide evidence that SOCS3 is a negative regulator of insulin signaling in skeletal muscle, liver, and adipose tissue. The ability of SOCS3 to inhibit insulin signaling suggests that these proteins influence energy balance and glucose homeostasis within the body. In support of this, SOCS3 is also known to have a role in the development of leptin resistance.

SOCS3 and leptin resistance

Leptin is a hormone produced and secreted by several tissues, which regulates energy balance and caloric intake in the body. Although adipose tissue is the principle site of leptin secretion, this hormone can also be released from skeletal muscle [51,52]. A change in both substrate availability and substrate requirements can modulate leptin secretion from these tissues, which results in the regulation of food intake and energy balance, stimulates glucose transport, and inhibits insulin secretion by pancreatic β-cells. The leptin receptor (LRb) is a class I cytokine receptor, and is membrane bound as a homodimer [53]. In the hypothalamus, leptin binds to its receptor on the plasma membrane, and this leads to tyrosine phosphorylation of Jak2, and subsequent tyrosine phosphorylation of LRb [54,55]. Phosphorylated LRb binds to, and activates STAT3 proteins. STAT3 activation increases pro-opiomelanocortin (POMC) expression, as well as inhibits neuropeptide Y (NPY) and agouti-related peptide (AgRP) activity, all resulting

in appetite suppression and increased energy expenditure [56-58]. The activation of STAT3 by leptin also mediates the transcription of SOCS3 protein [59]. Similar to IL-6 signal transduction, leptin induces SOCS3 expression, and SOCS3 then inhibits leptin signaling (Figure 1). SOCS3 inhibits leptin signaling by binding to Tyr985 on LRb, and blocking further signal transduction through STAT3, and also by inhibiting Jak2 phosphorylation[60,61]. Mice with haploinsufficiency of SOCS3 had lower plasma leptin levels, and had prolonged activation of STAT3 proteins compared to wild type mice when administered the same does of leptin [62]. When leptin was infused into neuron specific SOCS3 deficient mice, these mice had greater weight loss compared to the wild type mice. Furthermore, when these mice were fed a HFD, the wild type gained significantly more weight than the SOCS3 deficient mice [63]. SOCS3 mediated inhibition of leptin signaling prevents leptin from effectively modulating energy intake and suppressing appetite, and exacerbates obesity.

Under normal conditions, leptin stimulation results in increased activity of AMP activated protein kinase (AMPK), and downstream target acetyl-CoA carboxylase (ACC) in peripheral tissues [64]. AMPK is a regulator of cellular energy balance, and once activated switches on energy producing pathways. AMPK phosphorylates target proteins leading to increased fatty acid oxidation, glucose transport, and lipolysis in skeletal muscle, liver, and adipose tissue [65]. However, leptin failed to increase AMPK or ACC phosphorylation in rat soleus muscle following a HFD, indicating that the tissue had become leptin resistant [65,66]. Leptin stimulation resulted in decreased AMPK mediated Jak2, IRS-1, and Akt phosphorylation in the liver of rats fed a HFD compared

to control rats [67]. Additionally, AMPK expression was decreased in the HFD liver. Leptin resistance has also been connected to increased SOCS3 mRNA and protein expression in skeletal muscle cells [68]. When SOCS3 was overexpressed in skeletal muscle, there was decreased α2AMPK activity, and decreased ACC phosphorylation [69]. These results imply that increased SOCS3 can lead to the development of leptin resistance in the muscle cells.

Chronic low-grade inflammation is associated with both increased circulating IL-6 and leptin levels, and consequently increased SOCS3 expression. Therefore, SOCS3 expression has both direct and indirect effects on the insulin-signaling pathway under these conditions. As previously discussed, SOCS3 causes insulin resistance by directly inhibiting IR and IRS-1/IRS-2, which consequently causes decreased activity of downstream components in the insulin-signaling pathway. SOCS3 can also negatively regulate leptin signaling leading to impaired leptin induced glucose uptake via AMPK and insulin signaling, and cause subsequent interactions between the leptin and insulin signaling pathways (Fig. 1). These interactions allow SOCS3 to mediate further indirect effects on insulin signaling.

Physical activity and insulin signaling

It has been well documented that regular physical activity can alleviate or protect against T2D by enhancing insulin sensitivity in peripheral tissues [70-78]. Metformin is an antidiabetic drug that lowers fasting plasma insulin and glucose levels, and improves glucose tolerance by suppressing hepatic glucose production and increasing glucose uptake in skeletal muscle [79,80]. Metformin suppresses hepatic glucose production

through a reduction in the rate of gluconeogenesis [80]. Due to the effectiveness of metformin on lowering plasma glucose concentrations, and the inexpensive cost, metformin is the most commonly prescribed drug for T2D patients [81]. Studies comparing the effectiveness of exercise, metformin and the combination treatment on insulin sensitivity have yielded interesting findings. Insulin resistant individuals were either treated with metformin, underwent a single bout of exercise, or both combined, and insulin sensitivity was measured 4 hours post exercise. Euglycemic hyperinsulinemic clamp tests found that insulin sensitivity increased by 54% in the individuals that exercised, and these changes were not seen in the metformin or combination treatments [81]. When prediabetic individuals participated in exercise training with or without metformin for 12 weeks, insulin sensitivity was increased in all treatments. However, the increase in insulin sensitivity was 25-30% higher in the exercise without metformin treatment compared to the others [82]. Additionally, prediabetic individuals prescribed either metformin or 150 minutes of physical activity per week for approximately 3 years resulted in the incidence of diabetes being reduced by 31% and 58% in the metformin and physical activity groups respectively [83]. Life style changes associated with regular physical activity and treatment with metformin both enhance insulin sensitivity, and reduced the incidence of diabetes in high-risk candidates. Drugs are more often chosen as the prescribed treatment in T2D, however it has been shown that the endogenous response to physical activity is more effective. It is important to understand the mechanisms behind the increase in insulin sensitivity in response to physical activity, as well as, why these mechanisms are more effective than current pharmacological treatments.

IL-6 and physical activity

As previously stated, IL-6 is elevated during physical activity, and plasma levels increase up to 100 fold (Table 1). IL-6 infusion during physical activity caused increased glucose disposal [84], and stimulated the production of anti inflammatory cytokines IL-1 receptor antagonist and IL-10. The production of IL-10 is important because it inhibits the production of pro inflammatory cytokines IL-1, TNFα, and IL-8 [5,16,85]. Furthermore, glucose uptake rate was lower in IL-6 knockout mice compared to wild type, and the knockout mice did not benefit from voluntary wheel running to the same extent as the wild type mice [86]. These studies suggest that acute elevations in IL-6 increase insulin sensitivity, whereas the lack of IL-6 prevents the exercise induced increases in insulin sensitivity.

The mechanism by which elevated IL-6 improves insulin sensitivity following physical activity may involve the regulation of AMPK activity. AMPK is an evolutionary conserved αβγ heterotrimer that consists of an α catalytic subunit, and βγ regulatory subunits [87,88]. Mice that overexpressed a skeletal muscle specific kinase dead form of AMPKα2 had reduced exercise tolerance during a single bout of exercise compared to wild type mice [89,90]. Additionally, AMPKβ2 knock out mice had reduced maximal exercise capacity and AMPK activity during treadmill running compared to wild type mice [91], and muscle specific AMPKβ1β2 knock out mice showed decreased AMPKα1α2 activity and AMPK phosphorylation following exercise compared to wild type mice [92]. Following muscle contraction, glucose uptake rates did not increase until the last five minutes of the contraction period in hind limb muscles from AMPKα2

dominant negative mice, whereas glucose uptake rates increased rapidly and remained elevated throughout the contraction period in wild type mice [93]. A similar study on AMPKα2 dominant negative mice found that contraction induced glucose uptake was reduced by 50% in extensor digitorum longus muscle compared to the wild type mice, suggesting that AMPK activity has important role in physical activity induced glucose uptake [94]. However, another study found that contraction stimulated glucose uptake into tibialis anterior, extensor digitorum longus, and gastrocnemius muscles were similar in muscle specific transgenic mice with inactive AMPKα2 catalytic subunits when compared to wild type mice [95]. In order to visualize GLUT-4 translocation and localization, mice quadriceps muscle fibers were transfected with GLUT4-enhanced green fluorescent protein (EGFP). Following ablation of AMPKα2 activity in transgenic mice, GLUT4-EGFP basal localization, and contraction stimulated GLUT4-EGFP translocation was similar compared to wild type mice [96]. In contrast to above, these studies suggest that AMPKα2 activation may not be required for physical activity induced glucose uptake. Therefore, AMPK activity may be necessary for full activation of physical activity induced glucose transport, but it appears there are also AMPK independent mechanisms involved in this process [94].

Several studies have shown that IL-6 is an important factor involved in physical activity-mediated activation of AMPK. AMPK is activated by decreases in the energy state of the cell, or increases in the AMP: ATP ratio, and it was shown that incubation of skeletal muscle cells with IL-6 resulted in increased concentrations of AMP [97]. Incubating extensor digitorum longus muscle and cultured F442a adipocyte with IL-6 resulted in

increased AMPK and ACC phosphorylation in the cells [98,99]. Additionally, physical activity caused increased AMPK and ACC phosphorylation in skeletal muscle, liver, and adipose tissue of control mice, and these effects were diminished in IL-6 knockout mice [98,99]. IL-6 infusion into humans at a plasma concentration that mimics levels reached during strenuous exercise increased glucose disposal rate. Furthermore, L6 myotubes, when treated with IL-6, resulted in increased insulin stimulated translocation of GLUT-4 to the plasma membrane, and was accompanied by a 1.8-fold increase in AMPK phosphorylation compared to untreated myotubes [26]. Following adenoviral-mediated infection of myotubes with a dominant negative AMPKα subunit, IL-6 induced increases in insulin stimulated glucose uptake were inhibited. AMPK phosphorylation was reduced in obese rats compared to lean rats, and contraction failed to increase AMPK activity in the obese rats following exercise [100,101]. Similarly, HFD fed mice had reduced exercise tolerance, and attenuated AMPKα2 activity during a single bout of exercise compared to chow fed mice [102]. IL-6 has been shown to be required for physical activity-mediated increases in AMPK activity [98,99], but it remains unclear why IL-6 is inhibited from activating AMPK in response to physical activity in chronic inflammatory states. In contrast, it was found that T2D subjects had similar physical activity induced AMPKα2 activity compared to non-diabetic subjects [103]. However, none of these subjects were obese, and may not be suffering from chronic low-grade inflammation in conjunction with T2D. This interpretation was supported by another study that compared AMPK activity between obese non-diabetic, non-obese T2D, and obese T2D subjects. The obese non-diabetic and obese T2D subjects showed diminished physical activity induced increases in AMPK phosphorylation, AMPKα2 activity, and total AMPK

activity compared to non-obese T2D subjects [104]. Furthermore, obese non-diabetic and obese T2D subjects had attenuated increases in ACC phosphorylation compared to non-obese T2D subjects. These results indicate that the inhibition of physical activity induced increases in AMPK activity occurs under obese or chronic low-grade inflammatory conditions, and that IL- 6 resistance may be related to the reduced AMPK response.

Statement of Problem

The role of elevated IL-6 in insulin resistance and insulin sensitivity is an active area of investigation. The current literature provides evidence that IL-6 induces insulin resistance, and that it can also improve insulin sensitivity. These studies suggest that the effects of IL-6 on insulin signaling are context dependent, and that this is a critical factor in this paradox that cannot be overlooked.

Specific Aims

The purpose of the present study was to determine both the role of IL-6 on HFD induced glucose intolerance, and in response to voluntary physical activity in the prevention of insulin resistance in IL-6 deficient mice.

Hypotheses

1) IL-6 is required for HFD induced insulin resistance.
2) The absence of IL-6 will prevent the beneficial effects of physical activity on insulin signaling.

MATERIALS AND METHODS

Animals

The IL-6 knockout (KO) mice (B6.129S2-Il6^{tm1Kopf}/J) were purchased from Jackson Laboratory (Bar Harbour, ME, USA). The KO mice were generated using a targeting vector. This vector was designed to place a neomycin resistance cassette into the first coding exon of the IL-6 gene. This construct was electroporated into 129S2/SvPas-derived D3 embryonic stem cells. The correctly targeted embryonic stem cells were injected into wild type mice (C57BL/6J) blastocysts. The resulting mouse line was bred to C57BL/6J (Stock No. 000664) mice for 11 generations. Male KO (n=16), and wild type (WT) (n=14) were obtained at ~6 weeks of age, and studied after one week of acclimatization (Fig. 2). Mice were housed under controlled temperature (18-20°C), humidity (40-70%), decibel level (<70 dB), and lighting (12h of light; 12h of dark) with free access to food and water. All animal experiments were performed in accordance with the institutional animal care committee guidelines at Lakehead University.

Experimental protocol

The mice were fed a HFD (D12492; Research Diets Inc., New Brunswick, NJ, USA) containing the following nutrient content (in kcal percent): fat 60%, protein 20%, carbohydrate 20%; with a total caloric content of 5.24 kcal g^{-1} (Appendix A). Eight KO and 6 WT mice had free access to running wheels (Appendix B). Over the 4 weeks of the study, food intake and running distance were recorded daily, and body weight was recorded weekly (Fig. 2). Daily food intake was tracked by calculating the difference between the mass of food added to each cage, and the mass of food remaining in each cage. Daily running distances were tracked using CatEye Velo 5.

Delimitations

Delimitations are those set by the investigator.

1. The study subjects were mice and not humans
2. The study was one single time point

Limitations and Basic Assumptions

Limitations and basic assumptions are inherent to the experimental design.

1. Mice were disease and pathogen free
2. Mice were well fed and hydrated
3. The running distances were similar to the reading on the monitor (free spinning of the wheel as mice jump on and off was negligible)
4. There were no underlying factors within the skeletal muscles or liver that would affect normal function

Glucose tolerance test

After 3 weeks of HFD mice were morning fasted for 5 hours prior to the glucose tolerance test (GTT) (Fig. 2). Mice were secured in a tail-first restrainer with an adjustable head gate. This design allowed the animal to walk in to the restrainer without being physically forced backwards. Once secured, the tail was swabbed with alcohol soaked gauze to increase visibility of the vein. The lateral tail vein was then located in the middle third of the tail for blood draw. Baseline blood glucose levels were taken prior to a bolus intraperitoneal injection of glucose (1 g kg^{-1}). Blood samples were taken from the tail vein at baseline (0), and after 30, 60, 90, and 120 minutes. Glucose levels were measured with a hand held whole-blood glucose monitor (OneTouch Ultra2), and

values were compared at each time point. The blood glucose response was quantified by calculating the area under the curve after the injection of glucose and subtracting baseline to describe the concentration of glucose in the blood 120 minutes after administration.

Tissue collection

At the end of the 4 weeks, mice were morning fasted for 5 hours, and then insulin was administered intraperitoneally to all animals at a dose of 10 U kg^{-1}. Ten minutes after the insulin injection, mice were anesthetized with isofluorane, and the hearts were removed (Fig. 2). The liver, soleus, gastrocnemius/plantaris (combined) muscles (left and right leg muscles) were removed and immediately frozen in liquid nitrogen for further analysis. The gastrocnemius and plantaris muscles were combined because they both have similar type I and type II myosin heavy profiles (both have a predominant IIB, with varying type IIA and IIX), whereas the soleus is approximately 50% type I myosin heavy chain and is postural.

Tissue lysis

Soleus muscle

Frozen soleus muscles were homogenized in 20 volumes of ice-cold lysis buffer (25 mM Tris pH=7.5, 150mM NaCl, 1mM EDTA, 1% Triton-X 100) in 2 mL round bottom microcentrifuge tubes. Immediately before use, phosphatase inhibitor cocktails 2 (Sigma, P5726) and 3 (Sigma, P0044), and protease inhibitor cocktail (Sigma, P8340) were added to the lysis buffer at a final concentration of 1% (v/v). A tissue lyser bead was added to each tube, and the tubes were placed in pre-chilled cassettes. The tissues were disrupted

using the Qiagen Retsch TissueLyser for 3 min at 30 Hz. Samples were centrifuged at 16,000 x g for 10 minutes at 4°C, and then the supernatants were collected and stored at -80°C for immunoblot and enzyme-linked immunosorbent assay (ELISA) analysis.

Gastrocnemius and plantaris muscle

Frozen gastrocnemius/plantaris muscles were homogenized in 10 volumes of ice-cold lysis buffer (25 mM Tris pH=7.5, 150mM NaCl, 1mM EDTA, 1% Triton-X 100) in 2 mL round bottom microcentrifuge tubes. Immediately before use, sodium fluoride (NaF) (Sigma, S1504) was added as a serine/threonine phosphatase inhibitor at a final concentration of 20 mM, sodium orthovanadate ($NaVO_3$) (Abcam, ab120386) (Appendix C) was added as a tyrosine phosphatase inhibitor at a final concentration of 2 mM, and protease inhibitor cocktail (Sigma, P8340) was added to the lysis buffer at a final concentration of 1% (v/v). A tissue lyser bead was added to each tube, and the tubes were placed in pre-chilled cassettes. The tissues were disrupted using the Qiagen Retsch TissueLyser for 6 min at 30 Hz. Samples were centrifuged at 16,000 x g for 10 minutes at 4°C, and then the supernatants were collected and stored at -80°C for immunoblot and ELISA analysis.

Liver tissue

Frozen liver tissue was homogenized in 10 volumes of ice-cold lysis buffer (25 mM Tris pH=7.5, 150mM NaCl, 1mM EDTA, 1% Triton-X 100)) in 2 mL round bottom microcentrifuge tubes. Immediately before use, sodium fluoride (NaF) (Sigma, S1504) was added as a serine/threonine phosphatase inhibitor at a final concentration of 20 mM, sodium orthovanadate ($NaVO_3$) (Abcam, ab120386) was added as a tyrosine phosphatase

inhibitor at a final concentration of 2 mM, and protease inhibitor cocktail (Sigma, P8340) was added to the lysis buffer at a final concentration of 1% (v/v). A tissue lyser bead was added to each tube, and the tubes were placed in pre-chilled cassettes. The tissues were disrupted using the Qiagen Retsch TissueLyser for 6 min at 30 Hz. Samples were centrifuged at 16,000 x g for 10 minutes at 4°C, and then the supernatants were collected and stored at -80°C for immunoblot and ELISA analysis.

Cell culture

To serve as positive controls, C2C12 mouse skeletal muscle cells were grown in 25cm^2 or 75cm^2 flasks in a humidified incubator at 37°C, 5% CO_2, and 20% O_2. Flasks were coated for 30 minutes at room temperature with 0.1% filter sterilized gelatin (Knox) prior to cell seeding. For AICAR treatment, cells were grown for 2 days in growth media (GM, High Glucose Dulbecco's Modified Eagle's Medium (DMEM, Thermo Scientific, SH30022.01) containing 10% fetal bovine serum (FBS, Thermo Scientific, SH30396.03) and 1mM sodium pyruvate (Sigma, S8636)), after which the media was changed to differentiation media (DM, DMEM containing 0.05mg/ml gentamicin sulfate (Lonza, 17-518Z), 1mM sodium pyruvate, 2% donor equine serum (Thermo Scientific, SH30074.03), and 1% penicillin/streptomycin solution (Thermo Scientific, SV30010)) following a wash with Dulbecco's Phosphate Buffered Saline (DPBS, Thermo Scientific, SH30028.02) for 6 days. Media was changed to fresh DM every 2 days, and for the last 24 hours in culture, 1mM AICAR (Cayman Chemical, 10010241) was added to the flask in fresh DM. Alternatively, for insulin treatment, cells were cultured for one day in GM, after which media was changed to DM following a DPBS wash. Cells were grown for another 6 days in DM, and media was changed to fresh DM every 2 days. For the last 3

days in culture, humulin R (Lilly, H1-210) was added to the media in one flask to a concentration of 100nM to test the effects of chronically elevated insulin. In this flask, media was changed every day to fresh DM containing the humulin R. To assess acute responses to insulin, humulin R was added to a concentration of 100nM to a second flask 15 minutes before lysis.

Cell lysis

Cells were washed twice with DPBS, and ice-cold lysis buffer was added to the flask. The lysis buffer contained 25mM Tris (pH 7.5), 150mM sodium chloride, 1mM Ethylenediaminetetraacetic acid (EDTA), and 1% Triton X-100. Immediately before use, phosphatase inhibitor cocktails 2 (Sigma, P5726) and 3 (Sigma, P0044), and protease inhibitor cocktail (Sigma, P8340) were added to the lysis buffer at a final concentration of 1% (v/v). A cell scraper was used to remove the cells from the bottom of the flask, and the lysis buffer containing cells was removed from the flask and put into 2ml round bottom microcentrifuge tubes. A tissue lyser bead was added to each tube, and the samples were homogenized using the Qiagen Retsch TissueLyser for 2 minutes at 20Hz. The beads were removed and the samples were centrifuged at 10, 000 x g for 1 minute, after which the supernatant was collected, and the samples were stored at -80°C until the protein assay.

Protein quantification

Protein assays were done using Bio-Rad Protein Assay (Bio-Rad, Hercules CA, 500-0114) on all positive control cells, soleus muscle (diluted 1:5 in double distilled water), gastrocnemius/plantaris muscle (diluted 1:10 in double distilled water), and liver samples

(diluted 1:40 in double distilled water) to determine the protein concentrations of these samples for further use in western blotting and ELISA analysis. The protein assay standards were prepared from bovine serum albumin (BSA) at 1.45 mg/ml, which was then serially diluted to 0.09 mg/ml. The protein assay blank was double distilled water. Following the preparation of the standards and samples, 5 µl of the blank, each standard, and each sample were added to a separate well in duplicates. Reagent A' was prepared by combing 25 µl per well of Reagent A, and 20 µl of Reagent S for every 1 ml of Reagent A. 25 µl of Reagent A' was then added to each well, followed by 200 µl of Reagent B to each well. Once Reagent B was added to each well, the plate was sealed and put on the plate shaker for 5 seconds. The plate was incubated at room temperature for 15 minutes in the dark, and then read at 750 nm.

Sample preparation

All positive control cells, soleus muscle, gastrocnemius/plantaris muscle, and liver samples were prepared at a final concentration of 2.25 µg/µl. The final volume of 600 µl of each prepared sample was achieved by using 150 µl of 4X sodium dodecyl sulfate (SDS) reducing buffer (10 ml Tris (6.8 pH, 500 mM), 4.06 ml double distilled water, 2 g SDS, 5 mg bromophenol blue, 10 ml glycerol, 110 µl β-mercaptoethanol), and varying volumes of distilled water and sample supernatant depending on the initial protein concentration of each sample. These samples were prepared in 1.5 ml tubes, and were boiled for 5 minutes to denature the proteins.

Protein expression analysis

Gel electrophoresis

SDS-PAGE gels were made for protein analysis. First, a 15% separating (7.2 ml distilled water, 5 ml Tris (1.5 M, 8.8 pH), 0.2 ml 10% SDS, 7.5 ml 40% acrylamide) gel was made and the beaker was placed in a vacuum for 15 minutes to remove air bubbles. After the 15 minutes, the beaker containing the separating gel was removed from the vacuum, and 20 µl of 97% electrophoresis grade N, N, N', N'- tetramethylethylenediamine (TEMED) (Thermo Scientific, BP15020) and 100 µl of 10% ammonium persulfate (APS) (Bio-Rad, 1610700) were added on the stir plate mixing gently. The separating gel was poured to the 12 mm pour line from the bottom of the comb, and was overlayed with 20% methanol. This was allowed to polymerize for 30 minutes. After the gel polymerized, the methanol was washed out 3 times with 0.1% SDS, and the residue was dried with a Kim wipe. The stacking gel (12.7 ml distilled water, 5 ml Tris (0.5 M, 6.8 pH), 0.2 10% SDS, 2 ml 40% acrylamide) was made and the beaker was placed in a vacuum for 15 minutes to remove air bubbles and air from the solution. After 15 minutes, the beaker containing the stacking gel was removed from the vacuum, and 20 µl of 97% electrophoresis grade TEMED and 100 µl of 10% APS were added on the stir plate mixing gently. The stacking gel was poured, and the gel combs were inserted to make the wells for the samples. The gel was allowed to polymerize for 30 minutes. Once the gel had polymerized, a total of 45 µg of protein was loaded into each well, and the gel was run at 200V in 1X Running Buffer (3.0 g Tris base, 14.4 g glycine, 1.0 g SDS, 1.0 L distilled water) on ice for approximately 1 hour. Once the samples had run to the bottom of the gel, indicated once the dye front had disappeared, the electrophoresis was stopped.

Western blotting

The gel was transferred to nitrocellulose membranes at 30V overnight at 4°C in 1X Transfer Buffer (5.3 g Tris, 2.9 g glycine, 800 ml distilled water, 200 ml methanol). After the overnight transfer, the membranes were rinsed in distilled water for 5 minutes. Ponceau S stain solution (475 ml distilled water, 25 ml 5% acetic acid, 0.5 g (0.1 % w/v) Ponceau S) was added to the membranes for 5 minutes to reveal protein lanes, and verify equal loading. Ponceau S staining was used to verify equal loading over actin or other housekeeping protein detection because it is reversible, and it does not rely on a single protein for normalization. Therefore, it avoids the possibility that the housekeeping or actin protein used may vary in certain conditions, or that they can be saturated at the levels of loading necessary for the detection of low-expressed target proteins [105]. The membranes were then destained with 0.1M sodium hydroxide (NaOH) and washed for 5 minutes in 1X Tris-Buffered Saline with Tween 20 (TBST) (24.4 g Tris HCl, 5.56 g Tris base (pH 7.6), 87.66 g NaCl, 1 L distilled water, then 100 ml of this into 900 ml of distilled water and 1 ml Tween 20). The membranes were then blocked with the appropriate percentage of milk for 1 hour at room temperature. The membranes were then put into primary antibody solution (Antibodies diluted in milk. Used: phosphorylated Akt^{SER473} (0.125 mg/ml, Abcam), leptin (1 µg/ml, Abcam); pan Akt (1:1000 dilution, Cell Signaling Technology), SOCS3 (1:500 dilution, Cell Signaling Technology), phosphorylated $AMPK\alpha^{THR172}$ (1:500 dilution, Cell Signaling Technology), and total AMPKα (1:1000 dilution, Cell Signaling Technology)) overnight with agitation at 4°C. The next day the membranes were washed 5 times for 5 minutes each in 1X TBST. The membranes were incubated with goat-anti rabbit (HRP) secondary antibody

(Antibody diluted in milk. 1:2500 dilution, Thermo Scientific) for 1 hour at room temperature. Afterwards the membranes were washed again 5 times for 5 minutes each in 1X TBST. Chemiluminescence was done using Clarity Western ECL solution (Bio-Rad, 170-5060). Equal volumes of each solution were mixed together and the membranes were incubated in the solution for 5 minutes. The immunoreactive complexes were then detected with enhanced chemiluminescence (ChemiDoc^{TM} XRS, Bio-Rad, Hercules, CA, USA).

Normalization and densitometry

Each western was normalized to a loading control sample. The loading control sample was also used as a positive control to ensure that the antibody recognizes the targeted protein. The specific controls were: pAkt/total Akt (C2C12 myotubes treated with 100 nM dose of humulin R to mimic an acute dose of insulin for 15 minutes prior to cell lysis), pAMPKα/total AMPKα (C2C12 myotubes treated with 1 mM AICAR for 24 hours prior to cell lysis), and SOCS3/leptin (C2C12 myotubes treated with 100 nM dose of humulin R for 3 days to mimic a chronic dose of insulin prior to cell lysis). The protein bands were quantified by densitometry using ImageJ software.

Enzyme-linked immunosorbent assay

To quantify the endogenous levels of phosphorylated STAT3 in soleus muscle, gastrocnemius/plantaris muscle, and liver tissue, PathScan® Phospho-Stat3 (Tyr705) Sandwich ELISA Kit (Cell Signaling Technology, Danvers, MA, USA) was used as per manufacturer's manual. A total of 30 μg of protein was added to each well, and the plate was pre-coated with capture antibody. The plate was then sealed and incubated overnight

at 4°C. The next day the wells were washed 4 times with 200 µl of wash buffer each time. After the washes, 100 µl of the detection antibody solution was added to each well, and the plate was sealed and incubated for 1 hour at 37°C. The wells were then washed again 4 times with 200 µl of wash buffer each time. After the washes, 100 µl of HRP linked solution was added to each well, and the plate was sealed and incubated for 30 minutes at 37°C. The wells were then washed again 4 times with 200 µl of wash buffer each time. After the washes, 100 µl of 3,3', 5, 5'- tetramethylbenzidine (TMB) start solution was added to each well, and the plate was then sealed and incubated for approximately 10 minutes at 37°C. After the incubation, 100 µl of stop solution was added to each well, and the plate was read at 450 nm.

Statistics

Data are presented as means ± SEM. Comparisons between groups were done using two way analysis of variance (ANOVA) for all comparisons except average daily running distance (one way ANOVA), and the correlation of change in body weight and caloric intake. ANOVA tests were followed by Fisher LSD post-hoc tests (SigmaStat software, Systat, Chicago, IL, USA). Significance was accepted at $p \leq 0.05$.

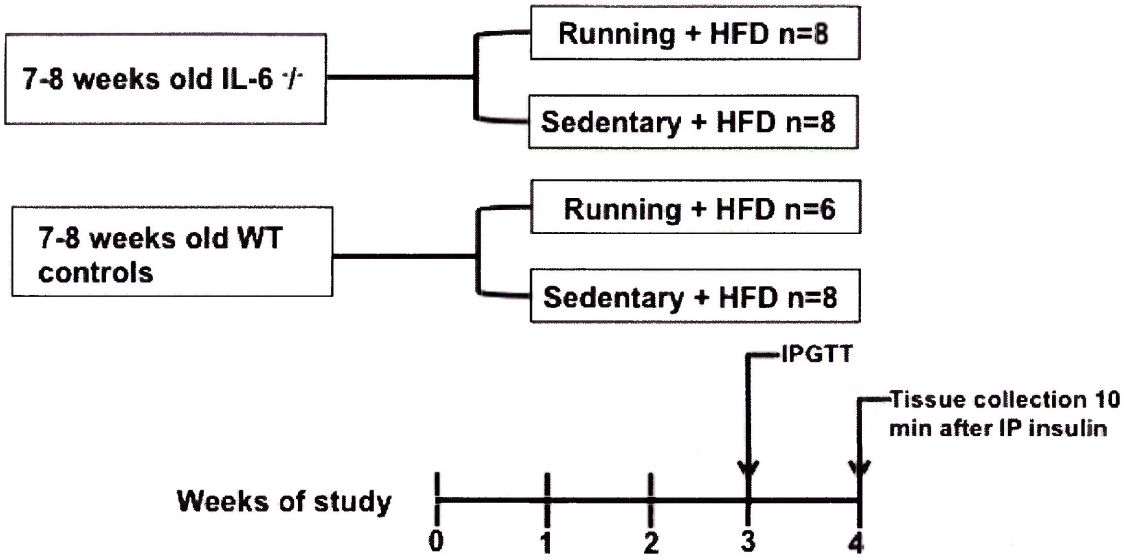

Figure 2. Flow chart of the study design. Abbreviations: HFD, high fat diet; IPGTT, intraperitoneal glucose tolerance test; IP, intraperitoneal; WT, wild type.

RESULTS

Sedentary mice showed increased weight gain compared to runners

Initial body weights of WT and KO mice, in both running (RUN) and sedentary (SED) groups were taken, and then recorded weekly for 4 weeks following the introduction of HFD (Fig. 3*A*). There were no differences in body weight between groups at the beginning of the study. As expected, WT SED mice gained more weight compared to RUN mice (24.8% *versus* 17.6%, $p<0.05$) (Fig. 3*A*). However, the KO mice showed no differences in weight gain between the SED and RUN groups ($p=0.08$) (Fig. 3*A*). Within WT, WT SED mice gained more weight compared to KO SED mice (24.8% *versus* 16.8%, $p<0.05$), but there were no differences in weight gain between the WT and KO mice in the RUN group ($p=0.08$) (Fig. 3*A*). Differences in body weight were observed between WT SED and KO RUN mice at week 1, 3, and 4 ($p<0.05$) (Fig. 3*B*). At week 4, WT SED mice had higher body weight compared to all other groups ($p<0.05$) (Fig. 3*B*).

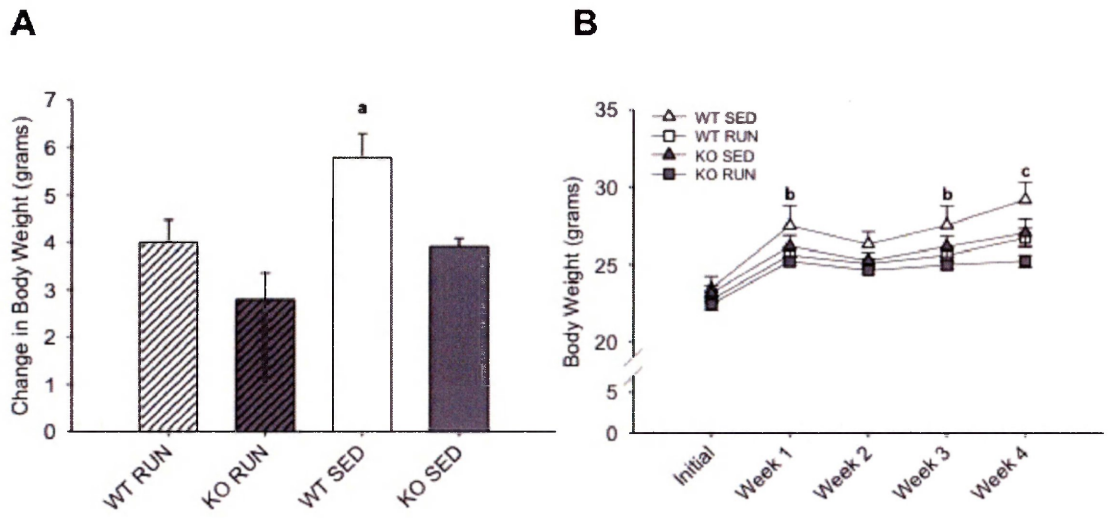

Figure 3. Sedentary mice showed increased weight gain compared to runners after 4 weeks on a high fat diet. A) The mean change in body weight (grams) in wild type (WT) and IL-6 knockout (KO) groups with (RUN) and without (SED) voluntary access to running wheels fed a high fat diet for 4 weeks. B) The mean body weight (grams) in WT and KO groups (RUN & SED) over 4 weeks on a high fat diet. [a] denotes significant differences ($p \leq 0.05$) between WT SED and all other groups. [b] denotes significant differences ($p \leq 0.05$) between WT SED and KO RUN groups. [c] denotes significant differences ($p \leq 0.05$) between WT SED and all other groups. Data are presented as mean ± SEM, (n=6-8 per group).

Runners consumed more calories compared to sedentary mice

Daily food intake was recorded over 4 weeks, and caloric intake of HFD was calculated (Fig. 4*A* and *B*). It was found that RUN mice consumed more calories compared to SED mice in both WT (13.0%, $p<0.05$) and KO (18.6%, $p<0.05$) groups (Fig 4*A*). By week 2, both KO RUN and WT RUN mice had increased cumulative caloric intake compared to both KO SED and WT SED mice ($p<0.05$), and this increase was also observed at week 3 and 4 (Fig. 4*B*). There were no differences in average daily running distance between these two groups over the duration of the study (10.3 km/day ± 0.7 *versus* 11.5 km/day ± 0.6, for WT and KO mice, respectively) ($p=0.083$) (Fig. 5*A*), and running distances remained constant over the 4 weeks (Fig. 5*B*).

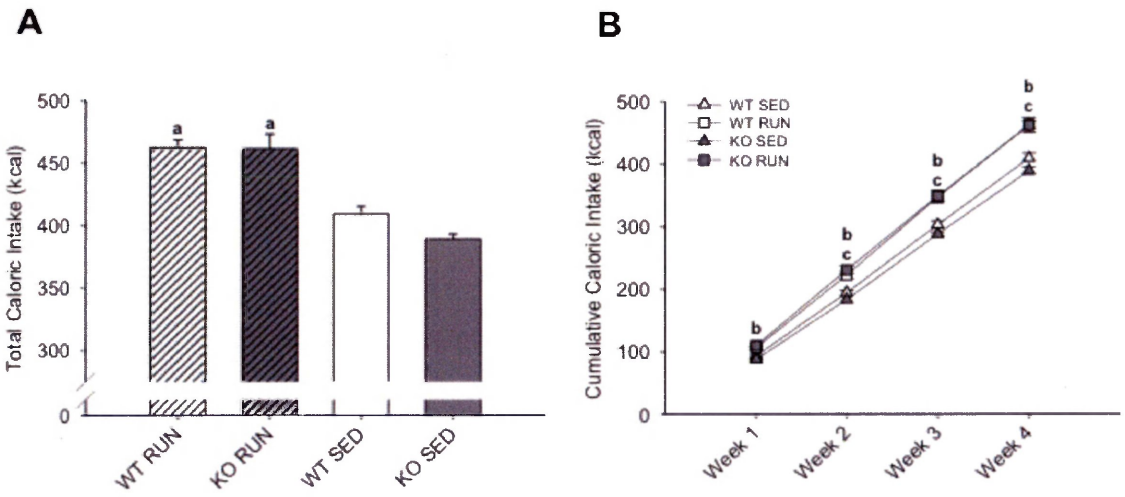

Figure 4. Runners consumed more calories compared to sedentary mice over 4 weeks on a high fat diet. A) The mean total caloric intake (kcal) for wild type (WT) and IL-6 knockout (KO) groups with (RUN) and without (SED) voluntary access to running wheels fed a high fat diet for 4 weeks. B) The mean cumulative caloric intake (kcal) for WT and KO groups (RUN & SED) over 4 weeks on a high fat diet. [a] denotes significant differences ($p \leq 0.05$) between RUN and SED mice. [b] denotes significant differences ($p \leq 0.05$) between KO RUN and both KO SED and WT SED groups. [c] denotes significant differences ($p \leq 0.05$) between WT RUN and both KO SED and WT SED groups. Data are presented as mean ± SEM, (n=6-8 per group).

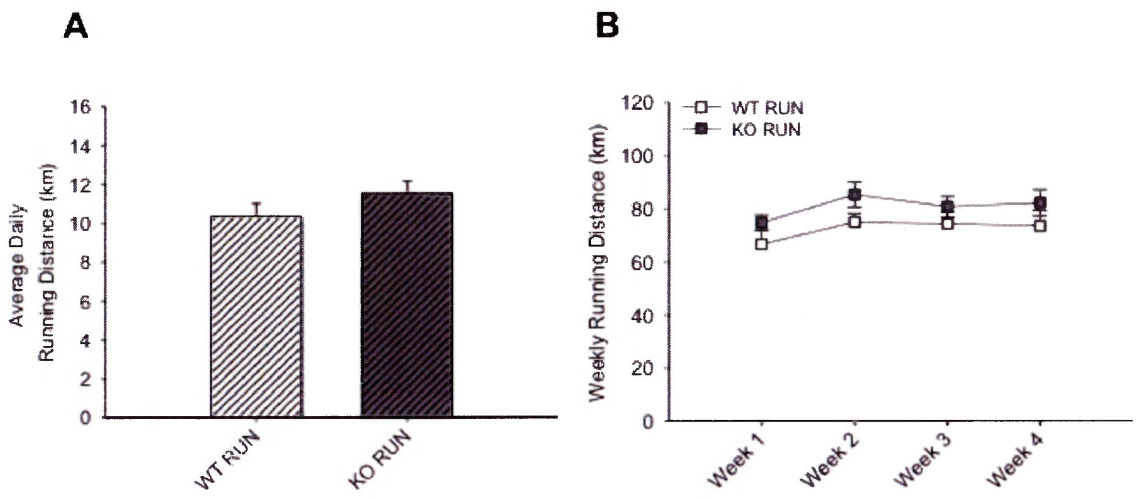

Figure 5. There were no differences in running distances between groups. A) The average daily running distance (km) for wild type (WT) and IL-6 knockout (KO) groups with (RUN) voluntary access to running wheels fed a high fat diet for 4 weeks. B) The mean weekly running distance (km) each week for WT and KO RUN groups fed a high fat diet for 4 weeks. Data are presented as mean ± SEM, (n=6-8 per group).

Lack of IL-6 negatively affects glucose tolerance in runners

After exposure to HFD for 3 weeks, there were no differences in fasting blood glucose levels between the groups (Fig. 6*A*). In order to test glucose tolerance, mice were given a bolus intraperitoneal injection of glucose and circulating glucose concentration was measured every 30 minutes for 2 hours. After 30 minutes, blood glucose levels were 25-30% higher ($p<0.05$) in the KO RUN compared to all other groups (Fig. 6*B*). The calculated area under the curve for the GTT yielded a non-significant (25.6%) increase in blood glucose in KO RUN compared to WT RUN (639 ± 56.6 *versus* 508.7 ± 66.9, $p=0.151$) (Fig. 6*C*).

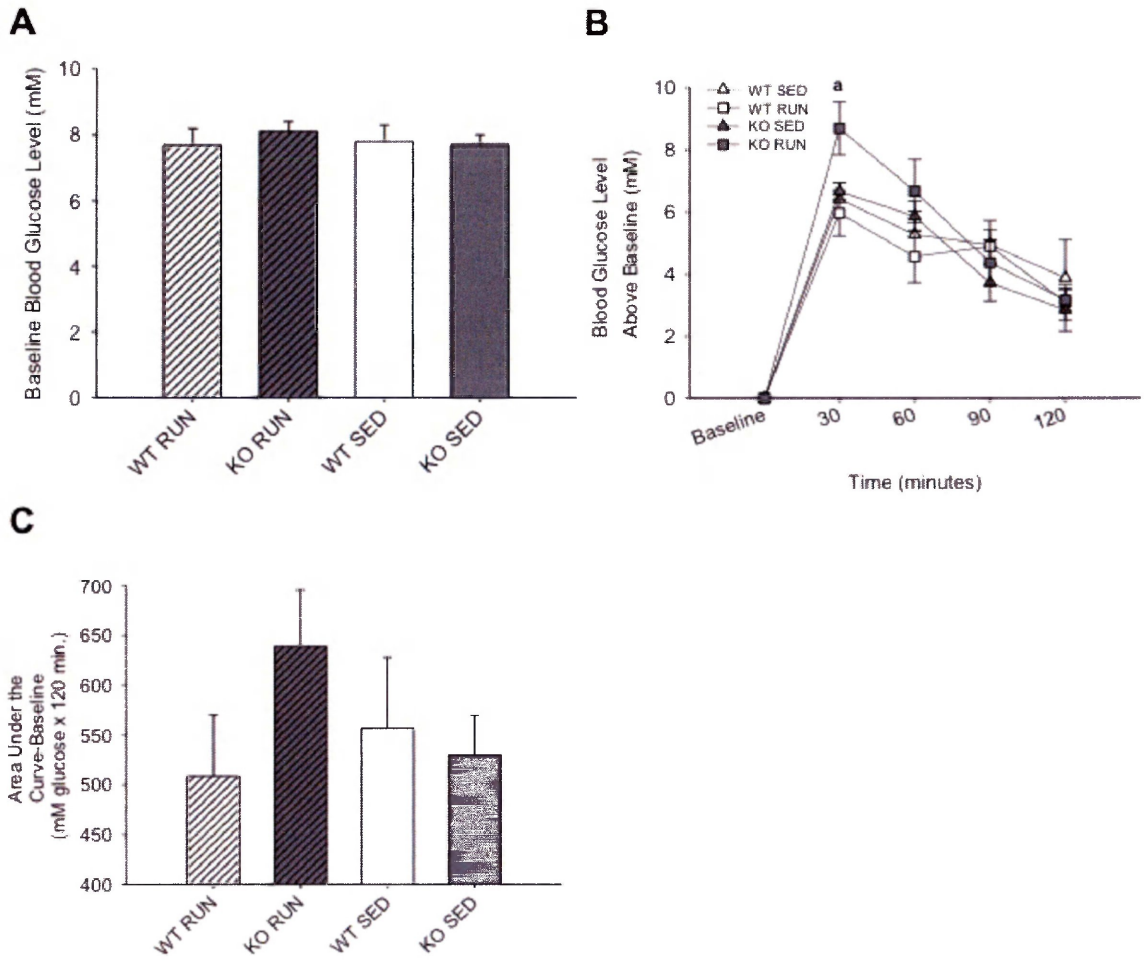

Figure 6. Lack of IL-6 negatively affects glucose tolerance in runners. A) The mean fasting (baseline) blood glucose level (mM) for wild type (WT) and IL-6 knockout (KO) groups with (RUN) and without (SED) voluntary access to running wheels after 3 weeks on a high fat diet. B) The mean blood glucose levels above baseline (mM) following a bolus intraperitoneal injection of glucose in WT and KO groups (RUN & SED) after 3 weeks on a high fat diet. C) The mean glucose area under the concentration-time curve above baseline (mM glucose x 120 minutes) for WT and KO groups (RUN & SED) after 3 weeks on a high fat diet. [a] denotes significant differences ($p \leq 0.05$) between KO RUN and all other groups. Data are presented as mean ± SEM, (n=6-8 per group).

Lack of IL-6 disrupts the link between caloric intake and weight gain in runners

The correlation between total caloric intake and weight gain was examined between WT RUN and KO RUN mice. As expected, the amount of weight gain was positively correlated (r^2=0.77) with total caloric intake in WT RUN mice over 4 weeks on HFD (Fig. 7). However, this association was absent in KO RUN mice (r^2=0.02), indicating an uncoupling of the caloric intake and weight gain relationship.

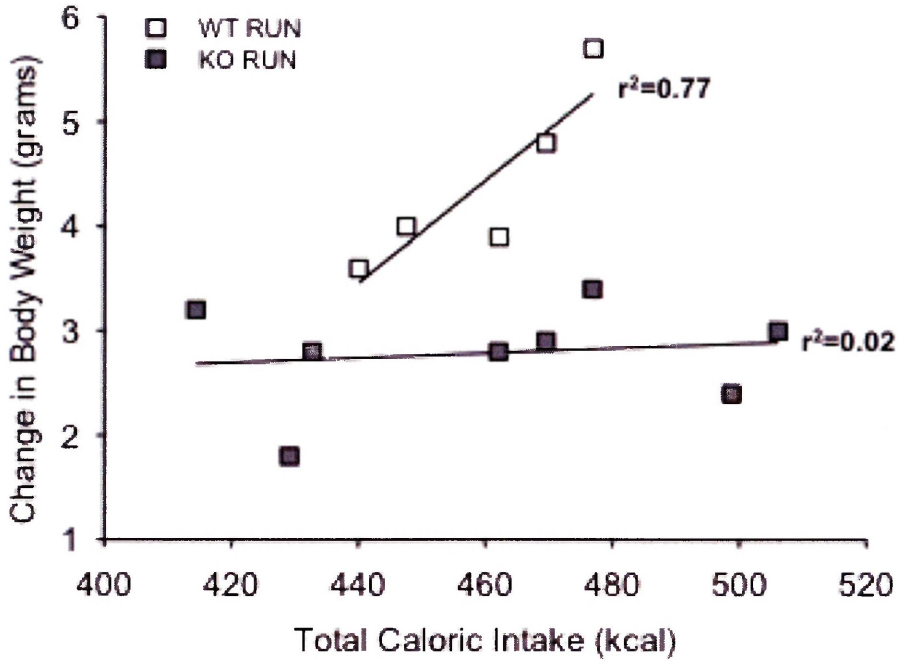

Figure 7. Lack of IL-6 disrupts the relationship between caloric intake and weight gain in runners. The correlation between total caloric intake (kcal) and total change in body weight (grams) in wild type (WT) (n=5) and IL-6 knockout (KO) (n=8) groups with (RUN) voluntary access to running wheels fed a high fat diet for 4 weeks. The data from one WT animal was removed as an outlier based on the value being greater than two standard deviations from the mean.

Phosphorylation and expression of signaling proteins

Soleus muscle

After 4 weeks on HFD, the phosphorylation and abundance of signaling proteins associated with insulin resistance, physical activity and IL-6 were determined in soleus muscle, gastrocnemius and plantaris muscles, and liver tissue. A bolus intraperitoneal injection of insulin was administered 10 minutes prior to tissue collection. In the soleus muscle, no differences in insulin stimulated Akt^{SER473} phosphorylation were found between groups (Fig. 8*A*). In soleus muscle, $STAT3^{TYR706}$ phosphorylation was decreased in KO RUN group compared to all other groups ($p<0.05$) (Fig. 8*B*). There was a 2-fold increase in SOCS3 expression in KO RUN compared to all other groups ($p<0.05$), supporting its inhibitory role for STAT3 (Fig. 8*C*). Leptin is a hormone produced and secreted by several tissues, which regulates energy balance and caloric intake in the body resulting in increased activity of AMP activated protein kinase (AMPK) in peripheral tissues [64]. AMPK phosphorylates target proteins leading to increased fatty acid oxidation, glucose transport, and lipolysis in skeletal muscle, liver, and adipose tissue [65]. It was found that leptin expression did not differ between groups in soleus muscle (Fig. 7*D*). $AMPK\alpha^{THR172}$ phosphorylation was not detected in any of the groups, and there were no differences in AMPKα expression between the groups (Fig. 8*E*).

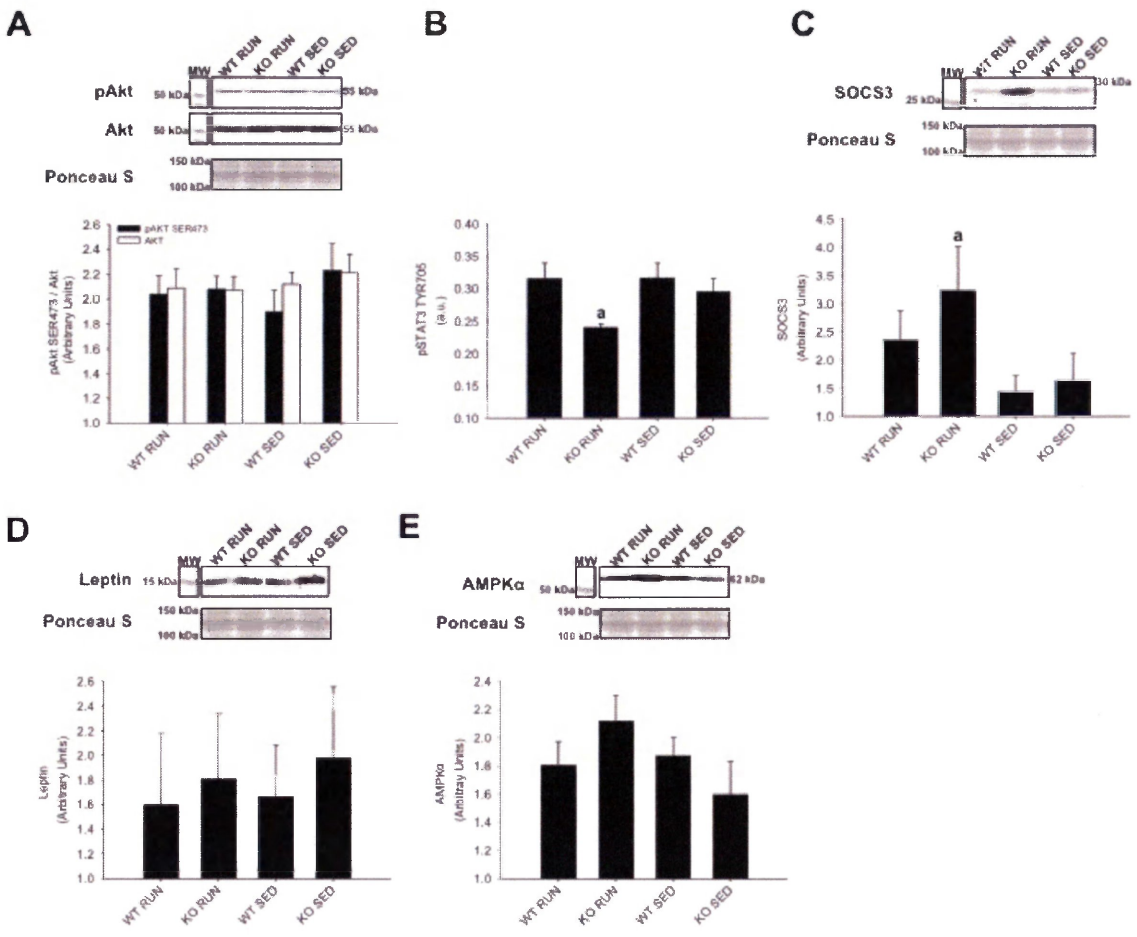

Figure 8. Soleus skeletal muscle protein expression of Akt, STAT3, SOCS3, leptin, and AMPKα from wild type (WT) and IL-6 knockout (KO) groups with (RUN) and without (SED) voluntary access to running wheels fed a high fat diet for 4 weeks. Insulin stimulated A) Akt^{SER473} phosphorylation B) $STAT3^{TYR706}$ phosphorylation C) SOCS3 expression D) Leptin expression E) AMPKα expression. [a] denotes significant differences ($p \leq 0.05$) between KO RUN and all other groups. Data are presented as mean ± SEM, (n=6-8 per group). Ponceau S stains are shown as markers of equal protein loading.

Gastrocnemius and plantaris muscle

In contrast to soleus muscle, insulin stimulated Akt^{SER473} phosphorylation was 31% higher in WT RUN compared to WT SED, but this effect of running was absent in KO mice in gastrocnemius/plantaris muscles ($p<0.05$) (Fig. 9*A*). There were no differences in $STAT3^{TYR706}$ phosphorylation between groups, and SOCS3 expression was not detected in any of the groups (Fig. 9*B*). However, there was a 2.4-fold increase in leptin expression in KO RUN compared to KO SED in gastrocnemius/plantaris muscles ($p<0.05$) (Fig. 9*C*). Similar to soleus muscle, $AMPK\alpha^{THR172}$ phosphorylation was not detected in any of the groups, and there were no differences in AMPKα expression between groups (Fig. 9*D*).

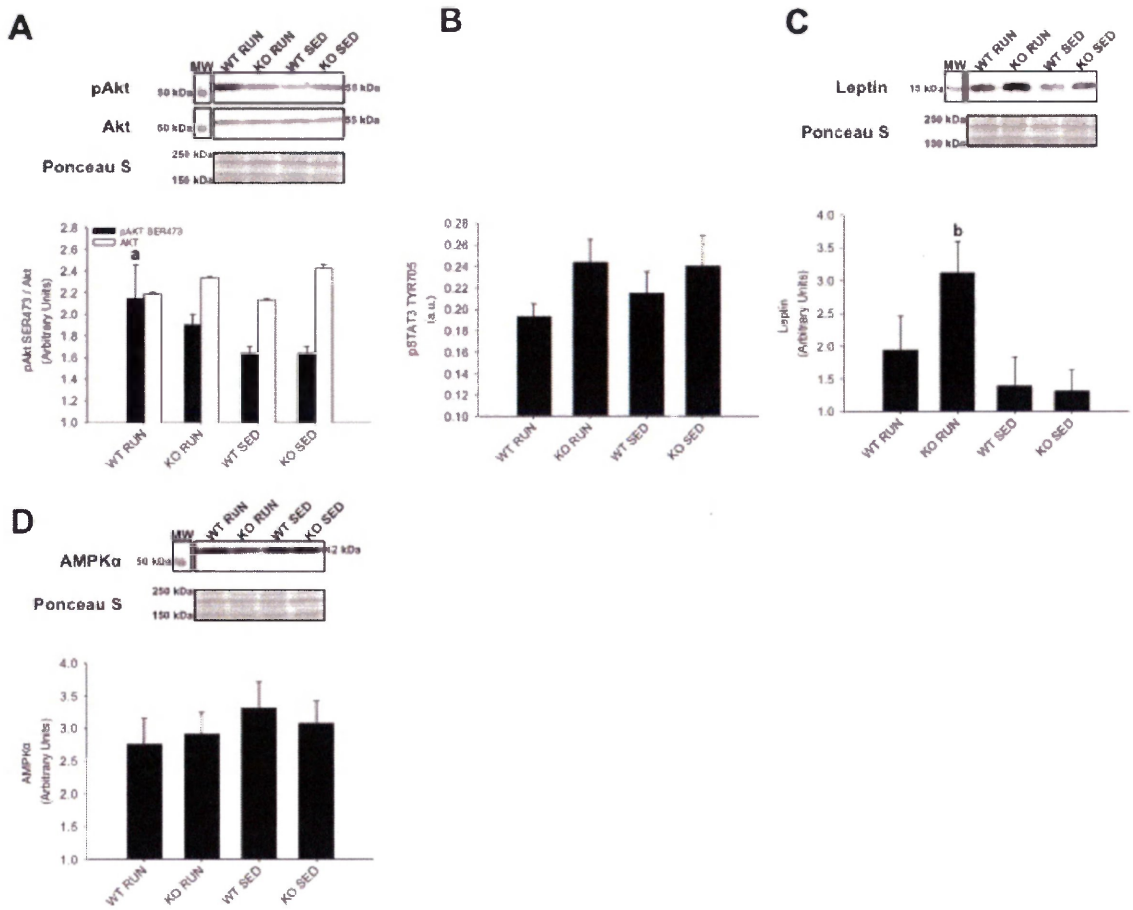

Figure 9. Gastrocnemius and plantaris skeletal muscle protein expression of Akt, STAT3, leptin, and AMPKα from wild type (WT) and IL-6 knockout (KO) groups with (RUN) and without (SED) voluntary access to running wheels fed a high fat diet for 4 weeks. Insulin stimulated A) Akt^{SER473} phosphorylation B) $STAT3^{TYR706}$ phosphorylation C) Leptin expression D) AMPKα expression. [a] denotes significant differences ($p \leq 0.05$) between WT RUN and WT SED groups. [b] denotes significant differences ($p \leq 0.05$) between KO RUN and KO SED groups. Data are presented as mean ± SEM, (n=6-8 per group). Ponceau S stains are shown as markers of equal protein loading.

Liver tissue

In liver, there were no differences in insulin stimulated Akt^{SER473} phosphorylation between groups (Fig. 10*A*). Similar to gastrocnemius/plantaris muscles, there were no differences in $STAT3^{TYR706}$ phosphorylation between groups (Fig. 10*B*). However, there was a 2-3.8-fold increase in SOCS3 expression in KO SED compared to all other groups ($p<0.05$) (Fig. 10*C*). No differences in leptin expression were found between groups ($p=0.268$ for WT RUN compared to KO RUN) (Fig. 10*D*). Unlike the skeletal muscles, $AMPK\alpha^{THR172}$ phosphorylation was detected in liver tissue. It was found that $AMPK\alpha^{THR172}$ phosphorylation was 27% higher in WT groups (both RUN and SED) compared to KO groups (both RUN and SED) ($p<0.05$) (Fig. 10*E*).

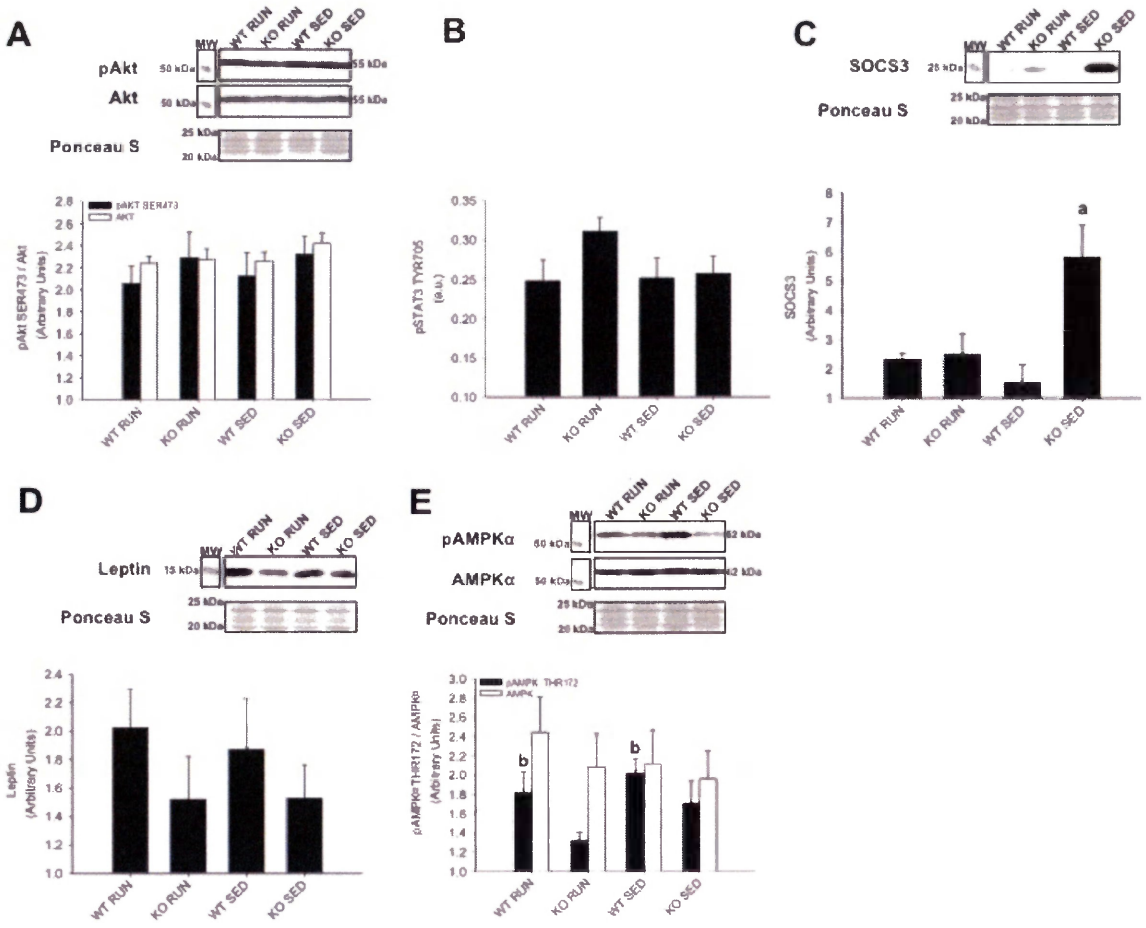

Figure 10. Liver protein expression of Akt, STAT3, SOCS3, leptin, and AMPKα from wild type (WT) and IL-6 knockout (KO) groups with (RUN) and without (SED) voluntary access to running wheels fed a high fat diet for 4 weeks. Insulin stimulated A) Akt^{SER473} phosphorylation B) STAT3^{TYR706} phosphorylation C) SOCS3 expression D) Leptin expression E) AMPKα^{THR172} phosphorylation. [a] denotes significant differences ($p \leq 0.05$) between KO SED and all other groups. [b] denotes significant differences ($p \leq 0.05$) between WT and KO groups. Data are presented as mean ± SEM, (n=6-8 per group). Ponceau S stains are shown as markers of equal protein loading.

DISCUSSION

It has been previously shown that IL-6 influences glucose and lipid metabolism, and more specifically, insulin action [106-108]. One intriguing aspect of IL-6 is the apparent context dependent dual role of this cytokine in glucose metabolism [109]. The present study was designed to investigate the role of IL-6 on HFD induced glucose intolerance, and the response to voluntary physical activity in the prevention of insulin resistance. Previous research has established that changes in the expression of SOCS3, and leptin, and the activation of STAT3, and AMPK are linked to the regulation of insulin signaling in obesity and diabetes [109]. This study was first to report that the lack of IL-6 disrupts the link between caloric intake and weight gain in runners, which provides new insight into the role of IL-6 in metabolism and energy storage. This study also revealed important tissue specific differences in SOCS3 expression, leptin expression, and Akt phosphorylation. In its entirety, the findings of the present study suggest that endogenous IL-6 is important for the prevention of insulin resistance induced by HFD.

During and up to 4 hours after exercise, plasma IL-6 concentrations can increase approximately 100 fold, which can increase insulin sensitivity in peripheral tissues [20,76]. Recent findings published by Benrick *et al.* (86) found that IL-6 KO mice with access to running wheels had increased blood glucose compared to WT mice with access to running wheels. The IL-6 KO mice did not benefit from running to the same extent as WT mice, and therefore, they concluded that endogenous IL-6 contributes to physical activity induced insulin sensitivity. While these findings are in agreement with the present study, there are some differences between the studies, including observations of

weight gain [86]. The study by Benrick *et al.* (86) utilized a voluntary physical activity model with HFD, and they found no differences in weight gain after 5 weeks on HFD between the WT and IL-6 KO mice, in either the sedentary or running groups. This was in contrast to the present study, which found that WT SED mice had increased weight gain compared to all other groups after 4 weeks on HFD. The HFD chosen for the present study contained a nutrient content of 60% fat, whereas the HFD used by Benrick *et al.* (86) contained 35.5% fat, which may account for the discrepancies in weight gain findings. Although it is known that HFD leads to increased IL-6, both the amount and duration of this increase is variable, and can lead to differences in insulin signaling. In long term studies without the use of HFD, blood glucose levels were increased in IL-6 KO mice compared to WT mice, and the IL-6 KO mice were obese at 9 months of age [108]. Previous studies that investigated the effects of HFD for 12-14 weeks also found that blood glucose levels were increased in IL-6 KO mice compared to WT mice [110,111]. Although these long duration studies demonstrated obesity and insulin resistance in the IL-6 KO mice, the experimental designs utilized overnight fasts and larger glucose doses to induce more robust effects. In an effort to detect early changes in glucose tolerance, and to assess insulin action within a more physiological context, the GTT was conducted after 3 weeks on HFD [112,113]. The mice were morning fasted for 5 hours to mimic an overnight fast in humans due to metabolic differences, and administered a conservative dose (1 g kg^{-1}) of glucose prior to the test [112]. The GTT revealed that blood glucose increased 25-30% more in KO RUN compared to all other groups after 30 minutes. Despite running equal distances, and consuming the same amount of calories, the KO RUN exhibited early signs of glucose intolerance compared

to WT RUN. This impaired glucose tolerance in KO RUN is an indicator of developing insulin resistance, and these findings suggest that IL-6 has an important role in the beneficial effects of physical activity on HFD induced glucose intolerance.

IL-6 has been shown to inhibit glycogen synthase activity and increase glycogen phosphorylase activity in rodent hepatocytes [114]. Additionally, IL-6 produced by contracting skeletal muscle may mediate hepatic glucose output during exercise, and when glucose was ingested prior to exercise, IL-6 release from skeletal muscle was attenuated [115,116]. In an IL-6 secreting tumour model, there was increased glycogen breakdown, which showed that IL-6 has a direct effect on glycogen metabolism in the liver [117]. In the present study, the amount of weight gain was positively correlated with total caloric intake in WT RUN mice, but this correlation was absent in KO RUN mice. The lack of endogenous IL-6 in KO RUN mice may have prevented effective glycogen breakdown in skeletal muscle and liver, which may have led to less glucose utilization during physical activity. Consequently, the KO RUN mice may have utilized available dietary fats as a main energy source. Although KO RUN were consuming similar amounts of food compared to WT RUN, utilizing fat as the primary energy substrate during physical activity may contribute to the disrupted relationship between weight gain and total caloric intake in KO RUN mice. Another possible explanation for these findings involves increased energy expenditure and thermogenesis in the KO RUN mice. Uncoupling proteins (UCPs) generate heat by uncoupling oxidative phosphorylation [118]. The increased expression of these proteins in brown adipose tissue (BAT) and white adipose tissue (WAT) result in increased energy expenditure, and

are involved in temperature and body weight regulation [118]. It has been shown that acute increases in IL-6 during physical activity can increase UCP1 expression in WAT, and UCP1 expression was lower in IL-6 KO compared to WT mice [119]. However, this physical activity induced increase in UCP1 expression was not completely blunted in IL-6 KO mice [119]. In the present study, the HFD may have prevented physical activity induced thermogenesis in WT RUN mice due to pro-inflammatory cytokines and other secreted factors associated with chronic low-grade inflammation, which can inhibit the expression of UCP1 in BAT and WAT [120]. Therefore, increased thermogenesis may have been blunted by HFD to a greater extent in WT RUN mice compared to the KO RUN mice leading to the uncoupling of the caloric intake-weight gain relationship.

It has been established that both the biochemical adaptations to exercise, and the effects of various dietary conditions differ between skeletal muscle types [121-123]. The results in this study provide novel support for different changes in early signaling pathways between oxidative and glycolytic skeletal muscles when exposed to HFD and physical activity. Increased SOCS3 expression has been associated with insulin resistance in peripheral tissues [36-38], but it has also been shown that physical activity can lead to increased SOCS3 mRNA expression [124]. Spangenburg *et al.* (124) found that exercise training increased SOCS3 mRNA expression in rat soleus and plantaris skeletal muscles, which may be linked to subsequent increases in IL-6 expression. Rat plantaris and mouse soleus muscle have comparable oxidative capacities measured by succinate dehydrogenase activity [125]. The present study demonstrated that the lack of IL-6 led to increased SOCS3 expression in response to physical activity in soleus muscle of KO

RUN mice. If increased SOCS3 expression contributes to increased IL-6 expression during physical activity, then KO RUN mice may have prevented a feed back mechanism on SOCS3, allowing SOCS3 expression to continue to increase in KO RUN compared to the other groups. Therefore, the present study demonstrates for the first time that physical activity can induce increases in SOCS3 expression at the protein level.

Insulin stimulates the activation of Akt causing the translocation of GLUT-4 vesicles to the plasma membrane, leading to glucose uptake in skeletal muscle [109]. Physical activity increases insulin sensitivity, while HFD has been shown to cause insulin resistance. The present study found increased insulin-stimulated Akt phosphorylation in WT RUN compared to WT SED mice, which demonstrated that physical activity prevented insulin resistance in gastrocnemius and plantaris muscles of WT RUN mice. However, insulin stimulated Akt phosphorylation in KO RUN mice was not increased compared to either SED group. This finding implies that the prevention of insulin resistance in response to physical activity requires endogenous IL-6 in skeletal muscle. It was hypothesized that KO mice may have impaired glycogen breakdown due to the lack of IL-6, resulting in a higher demand for free fatty acids. Since leptin can increase fatty acid uptake in skeletal muscle, the increased leptin expression in the gastrocnemius and plantaris muscles of KO RUN mice can possibly be explained due to the higher demand for free fatty acids in these muscles during physical activity [126,127]. If KO mice have restricted glucose availability, and are mainly utilizing fats, this resembles the high fat and low carbohydrate formulation of ketogenic diets. Increased leptin levels have been reported in rats that were fed a ketogenic diet compared to a standard diet, and these

findings provide additional support for increased leptin expression in the gastrocnemius and plantaris muscles due to the higher demand for free fatty acids [128].

Unlike in the soleus muscle, SOCS3 expression was not detected in the gastrocnemius and plantaris muscles in any of the groups. Additionally, no differences were observed in insulin stimulated Akt phosphorylation or leptin expression in the soleus muscle. The fiber differences between soleus, gastrocnemius, and plantaris muscles may account for the differences in SOCS3 expression, Akt phosphorylation, and leptin expression between the muscles. Mouse gastrocnemius and plantaris muscles have much higher percentage of myosin heavy chain IIB fibers, and glycolytic capacity compared to mouse soleus muscle [125]. While the gastrocnemius and plantaris muscles are recruited for voluntary wheel running, the soleus has higher oxidative capacity and is used both as a postural muscle, and for voluntary wheel running [129]. Therefore, the fiber type composition of these skeletal muscles and muscle recruitment may be important to the response of each muscle to HFD and physical activity.

In addition to the differential effects of exposure to HFD and physical activity on early signaling pathways in soleus, gastrocnemius, and plantaris muscles, the present study also found tissue specific effects in the liver. It was expected that HFD would lead to increased SOCS3 expression in the liver, and that this increase can be prevented by physical activity [109]. KO SED mice had increased SOCS3 expression compared to all other groups, but this increased SOCS3 was not associated with insulin resistance, as no differences in insulin stimulated Akt phosphorylation was observed between groups.

However, this finding may highlight impaired lipid metabolism in the liver of KO mice. Both WT RUN and WT SED mice had increased AMPK phosphorylation compared to both KO RUN and KO SED mice. The activation of AMPK in the liver leads to the stimulation of fatty acid oxidation, and the inhibition of lipogenesis [130]. The lack of IL-6 may impair AMPK phosphorylation causing lipid accumulation and increased SOCS3 expression in KO SED mice. While physical activity increases SOCS3 expression in skeletal muscle [124], increased SOCS3 expression is induced in the liver, and is linked to the pathogenesis of T2D [109]. It was shown that the lack of IL-6 induced early increases in SOCS3 expression in the liver in response to HFD in sedentary animals. However, in skeletal muscle, physical activity induced SOCS3 was exacerbated by the lack of IL-6, highlighting the tissue and context specific differences in SOCS3 expression.

CONCLUSION

In conclusion, the present study was designed to investigate the role of IL-6 on HFD induced glucose intolerance, and the response to voluntary physical activity in the prevention of insulin resistance in IL-6 deficient mice. The collective findings suggest that endogenous IL-6 is important for the prevention of insulin resistance induced by HFD. This study provides new insight into the role of the IL-6 in metabolism and energy storage, and highlights tissue specific changes in early signaling pathways in response to HFD for 4 weeks. There are many grave pathophysiological outcomes of T2D, including increased morbidity and mortality. Importantly, physical activity is effective in the prevention of T2D, and is more effective than current pharmacological treatments for

humans [81,82]. Therefore, it is critical to elucidate the mechanisms behind the increase in insulin sensitivity in response to regular physical activity.

Future directions

In light of the findings in the present study, an important future direction of this work would be to investigate the role of IL-6 on HFD induced glucose intolerance, and the response to voluntary physical activity in the prevention of insulin resistance using a long-term model. By extending the study from 4 weeks to 12 weeks, different effects of IL-6 on signaling pathways, and glucose metabolism may be found. These findings can be compared to the early changes that were detected after 4 weeks on HFD, which can continue to elucidate the mechanisms of IL-6 on insulin resistance and insulin sensitivity. Further understanding of these mechanisms has become especially important due to the introduction of the drug Tocilizumab. Tocilizumab is a recombinant humanized monoclonal antibody, which targets the IL-6 receptor. This drug is now prescribed for the treatment of rheumatoid arthritis in patients [131]. Tocilizumab has proven effective at treating this inflammatory disease, and therefore, it has been hypothesized that Tocilizumab may be beneficial in treating other inflammatory and chronic conditions, including T2D [131,132]. Studies have shown that Tocilizumab decreased insulin resistance in non-diabetic patients with rheumatoid arthritis, and decreased HbA1c levels in diabetic patients with rheumatoid arthritis [133,134]. While these studies have yielded positive results, much more rigorous clinical trials are necessary. IL-6 is important for physical activity induced increase in insulin sensitivity, and therefore, clinical trials are necessary since physical activity has been proven more effective than current pharmacological treatments for T2D. In order to test these effects, another possible

future direction could combine long-term HFD, physical activity, and Tocilizumab treatment. Instead of utilizing IL-6 KO mice, Tocilizumab could be administered to the mice in order to investigate the effects of this drug on insulin resistance and physical activity.

REFERENCES

1. Yenush L, Makati KJ, Smith-Hall J, Ishibashi O, Myers MG, Jr., et al. (1996) The pleckstrin homology domain is the principal link between the insulin receptor and IRS-1. J Biol Chem 271: 24300-24306.
2. Kido Y, Burks DJ, Withers D, Bruning JC, Kahn CR, et al. (2000) Tissue-specific insulin resistance in mice with mutations in the insulin receptor, IRS-1, and IRS-2. J Clin Invest 105: 199-205.
3. Hanke S, Mann M (2009) The phosphotyrosine interactome of the insulin receptor family and its substrates IRS-1 and IRS-2. Mol Cell Proteomics 8: 519-534.
4. Bjornholm M, Zierath JR (2005) Insulin signal transduction in human skeletal muscle: identifying the defects in Type II diabetes. Biochem Soc Trans 33: 354-357.
5. Starkie R, Ostrowski SR, Jauffred S, Febbraio M, Pedersen BK (2003) Exercise and IL-6 infusion inhibit endotoxin-induced TNF-alpha production in humans. FASEB J 17: 884-886.
6. Steensberg A, Fischer CP, Keller C, Moller K, Pedersen BK (2003) IL-6 enhances plasma IL-1ra, IL-10, and cortisol in humans. Am J Physiol Endocrinol Metab 285: E433-437.
7. Kado S, Nagase T, Nagata N (1999) Circulating levels of interleukin-6, its soluble receptor and interleukin-6/interleukin-6 receptor complexes in patients with type 2 diabetes mellitus. Acta Diabetol 36: 67-72.
8. Mohamed-Ali V, Goodrick S, Rawesh A, Katz DR, Miles JM, et al. (1997) Subcutaneous adipose tissue releases interleukin-6, but not tumor necrosis factor-alpha, in vivo. J Clin Endocrinol Metab 82: 4196-4200.
9. Fain JN, Madan AK, Hiler ML, Cheema P, Bahouth SW (2004) Comparison of the release of adipokines by adipose tissue, adipose tissue matrix, and adipocytes from visceral and subcutaneous abdominal adipose tissues of obese humans. Endocrinology 145: 2273-2282.
10. Weisberg SP, McCann D, Desai M, Rosenbaum M, Leibel RL, et al. (2003) Obesity is associated with macrophage accumulation in adipose tissue. Journal of Clinical Investigation 112: 1796-1808.
11. Bruunsgaard H (2005) Physical activity and modulation of systemic low-level inflammation. J Leukoc Biol 78: 819-835.
12. Kern PA, Ranganathan S, Li C, Wood L, Ranganathan G (2001) Adipose tissue tumor necrosis factor and interleukin-6 expression in human obesity and insulin resistance. Am J Physiol Endocrinol Metab 280: E745-751.

13. Jonsdottir IH, Schjerling P, Ostrowski K, Asp S, Richter EA, et al. (2000) Muscle contractions induce interleukin-6 mRNA production in rat skeletal muscles. J Physiol 528 Pt 1: 157-163.
14. Pedersen BK, Hoffman-Goetz L (2000) Exercise and the immune system: regulation, integration, and adaptation. Physiol Rev 80: 1055-1081.
15. Brandt C, Pedersen BK (2010) The role of exercise-induced myokines in muscle homeostasis and the defense against chronic diseases. J Biomed Biotechnol 2010: 520258.
16. Ostrowski K, Rohde T, Asp S, Schjerling P, Pedersen BK (1999) Pro- and anti-inflammatory cytokine balance in strenuous exercise in humans. J Physiol 515 (Pt 1): 287-291.
17. Pedersen BK, Steensberg A, Schjerling P (2001) Exercise and interleukin-6. Curr Opin Hematol 8: 137-141.
18. Pedersen BK, Steensberg A, Fischer C, Keller C, Keller P, et al. (2003) Searching for the exercise factor: is IL-6 a candidate? J Muscle Res Cell Motil 24: 113-119.
19. Steensberg A, van Hall G, Osada T, Sacchetti M, Saltin B, et al. (2000) Production of interleukin-6 in contracting human skeletal muscles can account for the exercise-induced increase in plasma interleukin-6. J Physiol 529 Pt 1: 237-242.
20. Pedersen BK, Febbraio MA (2012) Muscles, exercise and obesity: skeletal muscle as a secretory organ. Nat Rev Endocrinol 8: 457-465.
21. Pedersen BK (2012) Muscular interleukin-6 and its role as an energy sensor. Med Sci Sports Exerc 44: 392-396.
22. Moldoveanu AI, Shephard RJ, Shek PN (2000) Exercise elevates plasma levels but not gene expression of IL-1beta, IL-6, and TNF-alpha in blood mononuclear cells. J Appl Physiol 89: 1499-1504.
23. Pedersen BK, Akerstrom TC, Nielsen AR, Fischer CP (2007) Role of myokines in exercise and metabolism. J Appl Physiol 103: 1093-1098.
24. Taga T, Hibi M, Hirata Y, Yamasaki K, Yasukawa K, et al. (1989) Interleukin-6 triggers the association of its receptor with a possible signal transducer, gp130. Cell 58: 573-581.
25. Heinrich PC, Behrmann I, Muller-Newen G, Schaper F, Graeve L (1998) Interleukin-6-type cytokine signalling through the gp130/Jak/STAT pathway. Biochem J 334 (Pt 2): 297-314.
26. Carey AL, Steinberg GR, Macaulay SL, Thomas WG, Holmes AG, et al. (2006) Interleukin-6 increases insulin-stimulated glucose disposal in humans and glucose uptake and fatty acid oxidation in vitro via AMP-activated protein kinase. Diabetes 55: 2688-2697.
27. Glund S, Deshmukh A, Long YC, Moller T, Koistinen HA, et al. (2007) Interleukin-6 directly increases glucose metabolism in resting human skeletal muscle. Diabetes 56: 1630-1637.
28. Kim TH, Choi SE, Ha ES, Jung JG, Han SJ, et al. (2011) IL-6 induction of TLR-4 gene expression via STAT3 has an effect on insulin resistance in human skeletal muscle. Acta Diabetol.
29. Begue G, Douillard A, Galbes O, Rossano B, Vernus B, et al. (2013) Early activation of rat skeletal muscle IL-6/STAT1/STAT3 dependent gene expression in resistance exercise linked to hypertrophy. PLoS One 8: e57141.

30. Starr R, Willson TA, Viney EM, Murray LJ, Rayner JR, et al. (1997) A family of cytokine-inducible inhibitors of signalling. Nature 387: 917-921.
31. Endo TA, Masuhara M, Yokouchi M, Suzuki R, Sakamoto H, et al. (1997) A new protein containing an SH2 domain that inhibits JAK kinases. Nature 387: 921-924.
32. Naka T, Narazaki M, Hirata M, Matsumoto T, Minamoto S, et al. (1997) Structure and function of a new STAT-induced STAT inhibitor. Nature 387: 924-929.
33. Holmes AG, Mesa JL, Neill BA, Chung J, Carey AL, et al. (2008) Prolonged interleukin-6 administration enhances glucose tolerance and increases skeletal muscle PPARalpha and UCP2 expression in rats. J Endocrinol 198: 367-374.
34. Franckhauser S, Elias I, Rotter Sopasakis V, Ferre T, Nagaev I, et al. (2008) Overexpression of Il6 leads to hyperinsulinaemia, liver inflammation and reduced body weight in mice. Diabetologia 51: 1306-1316.
35. Rieusset J, Bouzakri K, Chevillotte E, Ricard N, Jacquet D, et al. (2004) Suppressor of cytokine signaling 3 expression and insulin resistance in skeletal muscle of obese and type 2 diabetic patients. Diabetes 53: 2232-2241.
36. Ueki K, Kondo T, Kahn CR (2004) Suppressor of cytokine signaling 1 (SOCS-1) and SOCS-3 cause insulin resistance through inhibition of tyrosine phosphorylation of insulin receptor substrate proteins by discrete mechanisms. Mol Cell Biol 24: 5434-5446.
37. Shi H, Tzameli I, Bjorbaek C, Flier JS (2004) Suppressor of cytokine signaling 3 is a physiological regulator of adipocyte insulin signaling. J Biol Chem 279: 34733-34740.
38. Shi H, Cave B, Inouye K, Bjorbaek C, Flier JS (2006) Overexpression of suppressor of cytokine signaling 3 in adipose tissue causes local but not systemic insulin resistance. Diabetes 55: 699-707.
39. Ueki K, Kadowaki T, Kahn CR (2005) Role of suppressors of cytokine signaling SOCS-1 and SOCS-3 in hepatic steatosis and the metabolic syndrome. Hepatol Res 33: 185-192.
40. Jorgensen SB, O'Neill HM, Sylow L, Honeyman J, Hewitt KA, et al. (2013) Deletion of skeletal muscle SOCS3 prevents insulin resistance in obesity. Diabetes 62: 56-64.
41. Palanivel R, Fullerton MD, Galic S, Honeyman J, Hewitt KA, et al. (2012) Reduced Socs3 expression in adipose tissue protects female mice against obesity-induced insulin resistance. Diabetologia 55: 3083-3093.
42. White MF, Livingston JN, Backer JM, Lauris V, Dull TJ, et al. (1988) Mutation of the insulin receptor at tyrosine 960 inhibits signal transmission but does not affect its tyrosine kinase activity. Cell 54: 641-649.
43. Zolotnik IA, Figueroa TY, Yaspelkis BB, 3rd (2012) Insulin receptor and IRS-1 co-immunoprecipitation with SOCS-3, and IKKalpha/beta phosphorylation are increased in obese Zucker rat skeletal muscle. Life Sci 91: 816-822.
44. Yaspelkis BB, 3rd, Kvasha IA, Figueroa TY (2009) High-fat feeding increases insulin receptor and IRS-1 coimmunoprecipitation with SOCS-3, IKKalpha/beta phosphorylation and decreases PI-3 kinase activity in muscle. Am J Physiol Regul Integr Comp Physiol 296: R1709-1715.

45. Senn JJ, Klover PJ, Nowak IA, Mooney RA (2002) Interleukin-6 induces cellular insulin resistance in hepatocytes. Diabetes 51: 3391-3399.
46. Senn JJ, Klover PJ, Nowak IA, Zimmers TA, Koniaris LG, et al. (2003) Suppressor of cytokine signaling-3 (SOCS-3), a potential mediator of interleukin-6-dependent insulin resistance in hepatocytes. J Biol Chem 278: 13740-13746.
47. Rui L, Yuan M, Frantz D, Shoelson S, White MF (2002) SOCS-1 and SOCS-3 block insulin signaling by ubiquitin-mediated degradation of IRS1 and IRS2. J Biol Chem 277: 42394-42398.
48. Kamura T, Sato S, Haque D, Liu L, Kaelin WG, Jr., et al. (1998) The Elongin BC complex interacts with the conserved SOCS-box motif present in members of the SOCS, ras, WD-40 repeat, and ankyrin repeat families. Genes & Development 12: 3872-3881.
49. Zhang JG, Farley A, Nicholson SE, Willson TA, Zugaro LM, et al. (1999) The conserved SOCS box motif in suppressors of cytokine signaling binds to elongins B and C and may couple bound proteins to proteasomal degradation. Proc Natl Acad Sci U S A 96: 2071-2076.
50. Yang SJ, Xu CQ, Wu JW, Yang GS (2010) SOCS3 inhibits insulin signaling in porcine primary adipocytes. Mol Cell Biochem 345: 45-52.
51. Wolsk E, Mygind H, Grondahl TS, Pedersen BK, van Hall G (2012) Human skeletal muscle releases leptin in vivo. Cytokine 60: 667-673.
52. Lappas M, Yee K, Permezel M, Rice GE (2005) Release and regulation of leptin, resistin and adiponectin from human placenta, fetal membranes, and maternal adipose tissue and skeletal muscle from normal and gestational diabetes mellitus-complicated pregnancies. J Endocrinol 186: 457-465.
53. Tartaglia LA (1997) The leptin receptor. J Biol Chem 272: 6093-6096.
54. Nakashima K, Narazaki M, Taga T (1997) Leptin receptor (OB-R) oligomerizes with itself but not with its closely related cytokine signal transducer gp130. FEBS Lett 403: 79-82.
55. Ghilardi N, Skoda RC (1997) The leptin receptor activates janus kinase 2 and signals for proliferation in a factor-dependent cell line. Mol Endocrinol 11: 393-399.
56. Schwartz MW, Woods SC, Porte D, Jr., Seeley RJ, Baskin DG (2000) Central nervous system control of food intake. Nature 404: 661-671.
57. Abdel-Malek ZA (2001) Melanocortin receptors: their functions and regulation by physiological agonists and antagonists. Cell Mol Life Sci 58: 434-441.
58. Benoit S, Schwartz M, Baskin D, Woods SC, Seeley RJ (2000) CNS melanocortin system involvement in the regulation of food intake. Horm Behav 37: 299-305.
59. Banks AS, Davis SM, Bates SH, Myers MG, Jr. (2000) Activation of downstream signals by the long form of the leptin receptor. J Biol Chem 275: 14563-14572.
60. Dunn SL, Bjornholm M, Bates SH, Chen Z, Seifert M, et al. (2005) Feedback inhibition of leptin receptor/Jak2 signaling via Tyr1138 of the leptin receptor and suppressor of cytokine signaling 3. Mol Endocrinol 19: 925-938.
61. Bjorbaek C, El-Haschimi K, Frantz JD, Flier JS (1999) The role of SOCS-3 in leptin signaling and leptin resistance. J Biol Chem 274: 30059-30065.
62. Howard JK, Cave BJ, Oksanen LJ, Tzameli I, Bjorbaek C, et al. (2004) Enhanced leptin sensitivity and attenuation of diet-induced obesity in mice with haploinsufficiency of Socs3. Nat Med 10: 734-738.

63. Mori H, Hanada R, Hanada T, Aki D, Mashima R, et al. (2004) Socs3 deficiency in the brain elevates leptin sensitivity and confers resistance to diet-induced obesity. Nat Med 10: 739-743.
64. Wolsk E, Mygind H, Grondahl TS, Pedersen BK, van Hall G (2011) The role of leptin in human lipid and glucose metabolism: the effects of acute recombinant human leptin infusion in young healthy males. Am J Clin Nutr 94: 1533-1544.
65. Martin TL, Alquier T, Asakura K, Furukawa N, Preitner F, et al. (2006) Diet-induced obesity alters AMP kinase activity in hypothalamus and skeletal muscle. J Biol Chem 281: 18933-18941.
66. Ritchie IR, Gulli RA, Stefanyk LE, Harasim E, Chabowski A, et al. (2011) Restoration of skeletal muscle leptin response does not precede the exercise-induced recovery of insulin-stimulated glucose uptake in high-fat-fed rats. Am J Physiol Regul Integr Comp Physiol 300: R492-500.
67. Brabant G, Muller G, Horn R, Anderwald C, Roden M, et al. (2005) Hepatic leptin signaling in obesity. FASEB J 19: 1048-1050.
68. Eguchi M, Gillis LC, Liu Y, Lyakhovsky N, Du M, et al. (2007) Regulation of SOCS-3 expression by leptin and its co-localization with insulin receptor in rat skeletal muscle cells. Mol Cell Endocrinol 267: 38-45.
69. Yang Z, Hulver M, McMillan RP, Cai L, Kershaw EE, et al. (2012) Regulation of insulin and leptin signaling by muscle suppressor of cytokine signaling 3 (SOCS3). PLoS One 7: e47493.
70. Ivy JL (1997) Role of exercise training in the prevention and treatment of insulin resistance and non-insulin-dependent diabetes mellitus. Sports Med 24: 321-336.
71. Borghouts LB, Keizer HA (2000) Exercise and insulin sensitivity: a review. Int J Sports Med 21: 1-12.
72. Hawley JA, Lessard SJ (2008) Exercise training-induced improvements in insulin action. Acta Physiol (Oxf) 192: 127-135.
73. Musi N, Goodyear LJ (2006) Insulin resistance and improvements in signal transduction. Endocrine 29: 73-80.
74. Hawley JA (2004) Exercise as a therapeutic intervention for the prevention and treatment of insulin resistance. Diabetes Metab Res Rev 20: 383-393.
75. Krisan AD, Collins DE, Crain AM, Kwong CC, Singh MK, et al. (2004) Resistance training enhances components of the insulin signaling cascade in normal and high-fat-fed rodent skeletal muscle. J Appl Physiol 96: 1691-1700.
76. Bradley RL, Jeon JY, Liu FF, Maratos-Flier E (2008) Voluntary exercise improves insulin sensitivity and adipose tissue inflammation in diet-induced obese mice. Am J Physiol Endocrinol Metab 295: E586-594.
77. Kiraly MA, Campbell J, Park E, Bates HE, Yue JT, et al. (2010) Exercise maintains euglycemia in association with decreased activation of c-Jun NH2-terminal kinase and serine phosphorylation of IRS-1 in the liver of ZDF rats. Am J Physiol Endocrinol Metab 298: E671-682.
78. Puppa MJ, White JP, Velazquez KT, Baltgalvis KA, Sato S, et al. (2012) The effect of exercise on IL-6-induced cachexia in the Apc (Min/+) mouse. J Cachexia Sarcopenia Muscle 3: 117-137.

79. DeFronzo RA, Barzilai N, Simonson DC (1991) Mechanism of metformin action in obese and lean noninsulin-dependent diabetic subjects. J Clin Endocrinol Metab 73: 1294-1301.
80. Hundal RS, Krssak M, Dufour S, Laurent D, Lebon V, et al. (2000) Mechanism by which metformin reduces glucose production in type 2 diabetes. Diabetes 49: 2063-2069.
81. Sharoff CG, Hagobian TA, Malin SK, Chipkin SR, Yu H, et al. (2010) Combining short-term metformin treatment and one bout of exercise does not increase insulin action in insulin-resistant individuals. Am J Physiol Endocrinol Metab 298: E815-823.
82. Malin SK, Gerber R, Chipkin SR, Braun B (2012) Independent and combined effects of exercise training and metformin on insulin sensitivity in individuals with prediabetes. Diabetes Care 35: 131-136.
83. Knowler WC, Barrett-Connor E, Fowler SE, Hamman RF, Lachin JM, et al. (2002) Reduction in the incidence of type 2 diabetes with lifestyle intervention or metformin. N Engl J Med 346: 393-403.
84. Febbraio MA, Hiscock N, Sacchetti M, Fischer CP, Pedersen BK (2004) Interleukin-6 is a novel factor mediating glucose homeostasis during skeletal muscle contraction. Diabetes 53: 1643-1648.
85. Ostrowski K, Schjerling P, Pedersen BK (2000) Physical activity and plasma interleukin-6 in humans--effect of intensity of exercise. Eur J Appl Physiol 83: 512-515.
86. Benrick A, Wallenius V, Asterholm IW (2012) Interleukin-6 mediates exercise-induced increase in insulin sensitivity in mice. Exp Physiol 97: 1224-1235.
87. O'Neill HM (2013) AMPK and Exercise: Glucose Uptake and Insulin Sensitivity. Diabetes Metab J 37: 1-21.
88. Cheung PC, Salt IP, Davies SP, Hardie DG, Carling D (2000) Characterization of AMP-activated protein kinase gamma-subunit isoforms and their role in AMP binding. Biochem J 346 Pt 3: 659-669.
89. Maarbjerg SJ, Jorgensen SB, Rose AJ, Jeppesen J, Jensen TE, et al. (2009) Genetic impairment of AMPKalpha2 signaling does not reduce muscle glucose uptake during treadmill exercise in mice. Am J Physiol Endocrinol Metab 297: E924-934.
90. Lee-Young RS, Griffee SR, Lynes SE, Bracy DP, Ayala JE, et al. (2009) Skeletal muscle AMP-activated protein kinase is essential for the metabolic response to exercise in vivo. J Biol Chem 284: 23925-23934.
91. Steinberg GR, O'Neill HM, Dzamko NL, Galic S, Naim T, et al. (2010) Whole body deletion of AMP-activated protein kinase {beta}2 reduces muscle AMPK activity and exercise capacity. J Biol Chem 285: 37198-37209.
92. O'Neill HM, Maarbjerg SJ, Crane JD, Jeppesen J, Jorgensen SB, et al. (2011) AMP-activated protein kinase (AMPK) beta1beta2 muscle null mice reveal an essential role for AMPK in maintaining mitochondrial content and glucose uptake during exercise. Proc Natl Acad Sci U S A 108: 16092-16097.
93. Abbott MJ, Bogachus LD, Turcotte LP (2011) AMPKalpha2 deficiency uncovers time dependency in the regulation of contraction-induced palmitate and glucose uptake in mouse muscle. J Appl Physiol 111: 125-134.

94. Lefort N, St-Amand E, Morasse S, Cote CH, Marette A (2008) The alpha-subunit of AMPK is essential for submaximal contraction-mediated glucose transport in skeletal muscle in vitro. Am J Physiol Endocrinol Metab 295: E1447-1454.
95. Fujii N, Hirshman MF, Kane EM, Ho RC, Peter LE, et al. (2005) AMP-activated protein kinase alpha2 activity is not essential for contraction- and hyperosmolarity-induced glucose transport in skeletal muscle. J Biol Chem 280: 39033-39041.
96. Lauritzen HP, Galbo H, Toyoda T, Goodyear LJ (2010) Kinetics of contraction-induced GLUT4 translocation in skeletal muscle fibers from living mice. Diabetes 59: 2134-2144.
97. Kelly M, Gauthier MS, Saha AK, Ruderman NB (2009) Activation of AMP-activated protein kinase by interleukin-6 in rat skeletal muscle: association with changes in cAMP, energy state, and endogenous fuel mobilization. Diabetes 58: 1953-1960.
98. Kelly M, Keller C, Avilucea PR, Keller P, Luo Z, et al. (2004) AMPK activity is diminished in tissues of IL-6 knockout mice: the effect of exercise. Biochem Biophys Res Commun 320: 449-454.
99. Ruderman NB, Keller C, Richard AM, Saha AK, Luo Z, et al. (2006) Interleukin-6 regulation of AMP-activated protein kinase. Potential role in the systemic response to exercise and prevention of the metabolic syndrome. Diabetes 55 Suppl 2: S48-54.
100. Sriwijitkamol A, Ivy JL, Christ-Roberts C, DeFronzo RA, Mandarino LJ, et al. (2006) LKB1-AMPK signaling in muscle from obese insulin-resistant Zucker rats and effects of training. Am J Physiol Endocrinol Metab 290: E925-932.
101. Barnes BR, Ryder JW, Steiler TL, Fryer LG, Carling D, et al. (2002) Isoform-specific regulation of 5' AMP-activated protein kinase in skeletal muscle from obese Zucker (fa/fa) rats in response to contraction. Diabetes 51: 2703-2708.
102. Lee-Young RS, Ayala JE, Fueger PT, Mayes WH, Kang L, et al. (2011) Obesity impairs skeletal muscle AMPK signaling during exercise: role of AMPKalpha2 in the regulation of exercise capacity in vivo. Int J Obes (Lond) 35: 982-989.
103. Musi N, Fujii N, Hirshman MF, Ekberg I, Froberg S, et al. (2001) AMP-activated protein kinase (AMPK) is activated in muscle of subjects with type 2 diabetes during exercise. Diabetes 50: 921-927.
104. Sriwijitkamol A, Coletta DK, Wajcberg E, Balbontin GB, Reyna SM, et al. (2007) Effect of acute exercise on AMPK signaling in skeletal muscle of subjects with type 2 diabetes: a time-course and dose-response study. Diabetes 56: 836-848.
105. Gilda JE, Gomes AV (2013) Stain-Free total protein staining is a superior loading control to beta-actin for Western blots. Anal Biochem 440: 186-188.
106. van Hall G, Steensberg A, Sacchetti M, Fischer C, Keller C, et al. (2003) Interleukin-6 stimulates lipolysis and fat oxidation in humans. J Clin Endocrinol Metab 88: 3005-3010.
107. Wallenius K, Wallenius V, Sunter D, Dickson SL, Jansson JO (2002) Intracerebroventricular interleukin-6 treatment decreases body fat in rats. Biochem Biophys Res Commun 293: 560-565.
108. Wallenius V, Wallenius K, Ahren B, Rudling M, Carlsten H, et al. (2002) Interleukin-6-deficient mice develop mature-onset obesity. Nat Med 8: 75-79.

109. Sarvas JL, Khaper N, Lees SJ (2013) The IL-6 Paradox: Context Dependent Interplay of SOCS3 and AMPK. J Diabetes Metab Suppl 13.
110. Di Gregorio GB, Hensley L, Lu T, Ranganathan G, Kern PA (2004) Lipid and carbohydrate metabolism in mice with a targeted mutation in the IL-6 gene: absence of development of age-related obesity. Am J Physiol Endocrinol Metab 287: E182-187.
111. Matthews VB, Allen TL, Risis S, Chan MH, Henstridge DC, et al. (2010) Interleukin-6-deficient mice develop hepatic inflammation and systemic insulin resistance. Diabetologia 53: 2431-2441.
112. Ayala JE, Samuel VT, Morton GJ, Obici S, Croniger CM, et al. (2010) Standard operating procedures for describing and performing metabolic tests of glucose homeostasis in mice. Dis Model Mech 3: 525-534.
113. McGuinness OP, Ayala JE, Laughlin MR, Wasserman DH (2009) NIH experiment in centralized mouse phenotyping: the Vanderbilt experience and recommendations for evaluating glucose homeostasis in the mouse. Am J Physiol Endocrinol Metab 297: E849-855.
114. Kanemaki T, Kitade H, Kaibori M, Sakitani K, Hiramatsu Y, et al. (1998) Interleukin 1beta and interleukin 6, but not tumor necrosis factor alpha, inhibit insulin-stimulated glycogen synthesis in rat hepatocytes. Hepatology 27: 1296-1303.
115. Febbraio MA, Steensberg A, Keller C, Starkie RL, Nielsen HB, et al. (2003) Glucose ingestion attenuates interleukin-6 release from contracting skeletal muscle in humans. J Physiol 549: 607-612.
116. Steensberg A, Febbraio MA, Osada T, Schjerling P, van Hall G, et al. (2001) Interleukin-6 production in contracting human skeletal muscle is influenced by pre-exercise muscle glycogen content. J Physiol 537: 633-639.
117. Metzger S GN, Barash V, Peretz T, Drize O, Shilyansky J, Shiloni E, Chajek-Shaul T (1997) Interleukin-6 secretion in mice is associated with reduced glucose-6-phosphatase and liver glycogen levels. Am J Physiol 273: E262-267.
118. Nedergaard J, Golozoubova V, Matthias A, Asadi A, Jacobsson A, et al. (2001) UCP1: the only protein able to mediate adaptive non-shivering thermogenesis and metabolic inefficiency. Biochim Biophys Acta 1504: 82-106.
119. Knudsen JG, Murholm M, Carey AL, Bienso RS, Basse AL, et al. (2014) Role of IL-6 in exercise training- and cold-induced UCP1 expression in subcutaneous white adipose tissue. PLoS One 9: e84910.
120. Sakamoto T, Takahashi N, Sawaragi Y, Naknukool S, Yu R, et al. (2013) Inflammation induced by RAW macrophages suppresses UCP1 mRNA induction via ERK activation in 10T1/2 adipocytes. Am J Physiol Cell Physiol 304: C729-738.
121. Holloszy JO BF (1976) Biochemical adaptations to endurance exercise in muscle. Annu Rev Physiol 38: 273-291.
122. Sharma N, Sequea DA, Castorena CM, Arias EB, Qi NR, et al. (2013) Heterogeneous effects of calorie restriction on in vivo glucose uptake and insulin signaling of individual rat skeletal muscles. PLoS One 8: e65118.

123. Blachnio-Zabielska A, Baranowski M, Zabielski P, Gorski J (2010) Effect of high fat diet enriched with unsaturated and diet rich in saturated fatty acids on sphingolipid metabolism in rat skeletal muscle. J Cell Physiol 225: 786-791.
124. Spangenburg EE, Brown DA, Johnson MS, Moore RL (2006) Exercise increases SOCS-3 expression in rat skeletal muscle: potential relationship to IL-6 expression. J Physiol 572: 839-848.
125. Bloemberg D, Quadrilatero J (2012) Rapid determination of myosin heavy chain expression in rat, mouse, and human skeletal muscle using multicolor immunofluorescence analysis. PLoS One 7: e35273.
126. Todd MK, Yaspelkis BB, 3rd, Turcotte LP (2005) Short-term leptin treatment increases fatty acids uptake and oxidation in muscle of high fat-fed rats. Metabolism 54: 1218-1224.
127. Steinberg GR, Dyck DJ, Calles-Escandon J, Tandon NN, Luiken JJ, et al. (2002) Chronic leptin administration decreases fatty acid uptake and fatty acid transporters in rat skeletal muscle. J Biol Chem 277: 8854-8860.
128. Thio LL, Erbayat-Altay E, Rensing N, Yamada KA (2006) Leptin contributes to slower weight gain in juvenile rodents on a ketogenic diet. Pediatr Res 60: 413-417.
129. Pellegrino MA, Brocca L, Dioguardi FS, Bottinelli R, D'Antona G (2005) Effects of voluntary wheel running and amino acid supplementation on skeletal muscle of mice. Eur J Appl Physiol 93: 655-664.
130. Viollet B, Foretz M, Guigas B, Horman S, Dentin R, et al. (2006) Activation of AMP-activated protein kinase in the liver: a new strategy for the management of metabolic hepatic disorders. J Physiol 574: 41-53.
131. Shetty A, Hanson R, Korsten P, Shawagfeh M, Arami S, et al. (2014) Tocilizumab in the treatment of rheumatoid arthritis and beyond. Drug Des Devel Ther 8: 349-364.
132. Tanaka T, Hishitani Y, Ogata A (2014) Monoclonal antibodies in rheumatoid arthritis: comparative effectiveness of tocilizumab with tumor necrosis factor inhibitors. Biologics 8: 141-153.
133. Ogata A, Morishima A, Hirano T, Hishitani Y, Hagihara K, et al. (2011) Improvement of HbA1c during treatment with humanised anti-interleukin 6 receptor antibody, tocilizumab. Ann Rheum Dis 70: 1164-1165.
134. Schultz O, Oberhauser F, Saech J, Rubbert-Roth A, Hahn M, et al. (2010) Effects of inhibition of interleukin-6 signalling on insulin sensitivity and lipoprotein (a) levels in human subjects with rheumatoid diseases. PLoS One 5: e14328.

APPENDIX A

Diet Induced Obesity (DIO) Diet

Product Data

D12492

OpenSource DIETS™

Description

Rodent Diet with 60% kcal% fat.

Used in Research

Obesity
Diabetes

Packaging

Product is packed in 12.5 kg box. Each box is identified with the product name, description, lot number and expiration date.

Lead Time

IN-STOCK. Ready for next day shipment.

Gamma-Irradiation

Yes. Add 10 days to delivery time.

Form

Pellet, Powder, Liquid

Shelf Life

Most diets require storage in a cool dry environment. Stored correctly they should last 3-6 months. Because of the high fat content is best if kept frozen.

Control Diets

D12450B

Formula

Product #		D12492	
		gm%	kcal%
Protein		26.2	20
Carbohydrate		26.3	20
Fat		34.9	60
	Total		100
	kcal/gm	5.24	

Ingredient	gm	kcal
Casein, 80 Mesh	200	800
L-Cystine	3	12
Corn Starch	0	0
Maltodextrin 10	125	500
Sucrose	68.8	275.2
Cellulose, BW200	50	0
Soybean Oil	25	225
Lard*	245	2205
Mineral Mix, S10026	10	0
DiCalcium Phosphate	13	0
Calcium Carbonate	5.5	0
Potassium Citrate, 1 H2O	16.5	0
Vitamin Mix, V10001	10	40
Choline Bitartrate	2	0
FD&C Blue Dye #1	0.05	0
Total	**773.85**	**4057**

Formulated by E. A. Ulman, Ph.D., Research Diets, Inc., 8/26/98 and 3/11/99.

*Typical analysis of cholesterol in lard = 0.95 mg/gram.
Cholesterol (mg)/4057 kcal = 232.8
Cholesterol (mg)/kg = 300.8

RESEARCH DIETS INC.
www.ResearchDiets.com

Research Diets, Inc.
20 Jules Lane
New Brunswick, NJ 08901
Tel: 732.247.2390
Fax: 732.247.2340
info@researchdiets.com

APPENDIX B

Running Wheel Set Up

Running wheels (4.5 inch Run Around Wheels) were suspended from the top of the cage. A magnet was attached to the running wheel, and the CatEye Velo 5 sensor was suspended through a light switch cover. The purpose of the light switch cover was to prevent the mice from chewing on the wires. The CatEye Velo 5 sensor tracked wheel revolutions, and distance was adjusted based on wheel circumference.

APPENDIX C

Sodium Orthovanadate Protocol

200 mM (100X) stock solution of sodium orthovanadate (Abcam, ab120386) was prepared to be used a tyrosine phosphatase inhibitor during tissue lysis. First, 3.68 g of sodium orthovanadate was added to 90 ml of double distilled water, and the solution was mixed on a stir plate. As the solution was mixing, the volume was brought to 100 ml. Once the solution was mixed thoroughly, the initial pH of the solution was checked. The solution was then brought to pH=10 using 12N/1N hydrochloric acid (HCl). During the pH process the solution turned yellow, and then orange. The solution was then microwaved for 60 seconds until it began to boil, and the solution turned colourless. The colourless solution was then cooled to room temperature. Once at room temperature, the solution was again brought to pH=10 using 12N/1N HCl. During the pH process the solution yellow. The solution was then microwaved for 60 seconds until it began to boil, and the solution turned colourless. The colourless solution was then cooled to room temperature. Once at room temperature, the solution was again brought to pH=10 using 12N/1N HCl. During the pH process the solution turned very pale yellow. The solution was then microwabed for 60 seconds until it began to boil, and the solution turned colourless. The colourless solution was then cooled to room temperature. Once at room temperature, the solution was again brought to pH=10 using 12N/1N HCl. The pH was stabilized at 10, and the solution remained colourless. The sodium orthovanadate solution was then stored in 1 ml aliquots at -20 °C.